広島大学学位請求論文

Functional analysis of a cis-regulatory element of *sonic hedgehog* gene in newt limb regeneration

（イモリ四肢再生におけるソニックヘッジホッグ遺伝子シス調節エレメントの機能解析）

2019 年

広島大学大学院理学研究科

数理分子生命理学専攻

鈴木　美有紀

目次

１．主論文

Functional analysis of a cis-regulatory element of *sonic hedgehog* gene in newt limb regeneration
(イモリ四肢再生におけるソニックヘッジホッグ遺伝子シス調節エレメントの機能解析)

２．公表論文

Suzuki, M., Hayashi, T., Inoue, T., Agata, K., Hirayama, M., Shigenobu, S., Takeuchi, T., Yamamoto, T. and Suzuki, K. T. (2018). Cas9 ribonucleoprotein complex allows direct and rapid analysis of coding and noncoding regions of target genes in *Pleurodeles waltl* development and regeneration. *Dev Biol* **443**, 127-136.

３．参考論文

(1) **Miyamoto, K., Suzuki, K. T., Suzuki, M., Sakane, Y., Sakuma, T., Herberg, S., Simeone, A., Simpson, D., Jullien, J., Yamamoto, T., et al.** (2015). The Expression of TALEN before Fertilization Provides a Rapid Knock-Out Phenotype in *Xenopus laevis* Founder Embryos. *PLoS One* **10**, e0142946.

(2) **Suzuki, M., Takagi, C., Miura, S., Sakane, Y., Sakuma, T., Sakamoto, N., Endo, T., Kamei, Y., Sato, Y., Kimura, H., et al.** (2016). *In vivo* tracking of histone H3 lysine 9 acetylation in *Xenopus laevis* during tail regeneration. *Genes Cells* **21**, 358-369.

(3) **Suzuki, K. T., Suzuki, M., Shigeta, M., Fortriede, J. D., Takahashi, S., Mawaribuchi, S., Yamamoto, T., Taira, M. and Fukui, A.** (2017). Clustered *Xenopus* keratin genes: A genomic, transcriptomic, and proteomic analysis. *Dev Biol* **426**, 384-392.

(4) **Suzuki, K. T., Sakane, Y., Suzuki, M. and Yamamoto, T.** (2018). A Simple Knock-In System for *Xenopus* via Microhomology Mediated End Joining Repair. *Methods Mol Biol* **1865**, 91-103.

主　論　文

Functional analysis of a cis-regulatory element of *sonic hedgehog* gene in newt limb regeneration

Miyuki Suzuki

Department of Mathematical and Life Sciences

Graduate School of Science

Hiroshima University

2019

Contents

GENERAL INTRODUCTION

Urodele amphibians can functionally and morphologically regenerate their organs, such as limb, eye, heart, tail, and brain (Parish et al. 2007; Barbosa-Sabanero et al. 2012; Inoue et al. 2012; Leone et al. 2015; Tsutsumi et al. 2015; Stocum 2017). In particular, limb regeneration has been extensively studied to decipher the mechanisms underlying the remarkable capability of organ regeneration (Brockes and Kumar 2002; Bryant et al. 2002; Suzuki et al. 2006; Tanaka 2016). Successful limb regeneration requires a blastema, which consists of multipotent mesenchymal stem cells (known as blastema cells). After amputation, keratinocytes from the stump migrate and cover the surface and then form the wound epidermis. Blastema cells arise from dedifferentiation of stump tissues such as dermis, muscle, cartilage, bone, and connective tissues (Stocum 2012). Apical thickened wound epidermis, called the apical epidermal cap (AEC), and nerves are crucial for blastema growth and maintenance (Thornton 1956; Mescher 1976; Singer & Craven 1948; Pirotte et al. 2016). However, the molecular mechanisms behind regeneration, such as the factors responsible for blastema formation and patterning, have not been clarified.

Iberian ribbed newt as an emerging model organism for regenerative biology

Newts have remarkable ability to regenerate their organs and have been used in research for centuries. However, molecular genetic research in newt has been hampered by difficulties in breeding and the lack of a simple and efficient method for gene modification. To overcome this issue, researchers recently adopted Iberian ribbed newt, *Pleurodeles waltl*, as a suitable laboratory model (Elewa et al. 2017; Hayashi et al. 2013). *P. waltl* can

be bred easily and reaches sexual maturity in 6 (male) or 9 months (female); in addition, fertilized eggs can be obtained every 2 weeks throughout the year. Recently, the genome sequence of *P. waltl* was obtained and edited using clustered regularly interspaced short palindromic repeat (CRISPR)-CRISPR associated (Cas) technology, providing a foundation for comparative genomic and regeneration studies (Elewa et al. 2017).

Genome editing in amphibians

CRISPR-Cas-based genome editing has been established as an efficient and simple system for gene disruption in many species, such as *Caenorhabditis elegans* (Lo et al. 2013), *Drosophila melanogaster* (Bassett et al. 2013), zebrafish (Chang et al. 2013; Hwang et al. 2013), medaka (Ansai and Kinoshita 2014), mouse (Shen et al. 2013; Wang et al. 2013), and rat (Li et al. 2013). It also allowed functional investigations in nonmodel organisms, such as mosquito (Kistler et al. 2015), salmon (Edvardsen et al. 2014), and pig (Burkard et al. 2017). In amphibians, the effectiveness of CRISPR-Cas has been reported in *Xenopus tropicalis* and *Xenopus laevis* (Nakayama et al. 2013; Wang et al. 2015; Shigeta et al. 2016).

Recently, it was reported that a premixture of recombinant Cas9 protein and guide RNA (gRNA), which forms a ribonucleoprotein complex (RNP), more efficiently introduced mutation in virtually all somatic cells in injected founder embryos in zebrafish, designated as crispants (Burger et al. 2016). Sakane et al. also demonstrated that Cas9 RNP can effectively disrupt genes, with associated somatic mutation rates reaching ~100% in *X. tropicalis* crispants (Sakane et al. 2018). In urodeles, although several groups have reported successful gene knockout using Cas9 mRNA and gRNA (Flowers et al.

2014; Fei et al. 2014; Bryant et al. 2017; Elewa et al. 2017), the effectiveness of Cas9 RNP has not been validated, and more efficient gene knockout methods are required for direct and rapid phenotyping analysis in the F_0 generation.

Role of sonic hedgehog signaling in limb development and regeneration

The patterning of developing limb is directed by signaling across the three axes: proximal–distal, dorsal–ventral, and anterior–posterior. The posterior region of forming limb bud is referred to as the zone of polarizing activity (ZPA) exclusively expressing *Sonic hedgehog* (*Shh*) and it mediates signaling along the anterior–posterior axis of developing limb. ZPA and SHH are active in inducing polydactyly upon grafting or misexpression at the anterior region of limb bud (Tickle et al. 1975; Riddle et al. 1993; Lopez-Martinez et al. 1995; Yang et al. 1997). In addition, mice with *Shh* knockout display severe deficiency in the anterior–posterior patterning of their autopods (Chiang et al. 1996; Chiang et al. 2001).

shh is also expressed in the posterior mesenchyme of developing and regenerating limbs of amphibians (Endo et al. 1997; Torok et al. 1999). Inhibition of Shh signaling with a Smoothened inhibitor, cyclopamine, leads to incomplete digital development in the regenerating limbs (Roy and Gardiner 2002; Stopper and Wagner 2007). Furthermore, overexpression of *shh* in the anterior mesenchyme of regenerating limbs induces polydactyly (Roy et al., 2000). Therefore, Shh has a morphogenetic property in patterning the anterior–posterior axis, even in regenerating urodele limbs.

Zone of polarizing activity regulatory sequence (ZRS): Limb-specific enhancer of shh

Among vertebrates, the ZPA regulatory sequence of *Shh* (ZRS, also known as MFCS1: Lettice et al. 2003; Sagai et al. 2005) is a highly conserved 800-bp element that is located at an intron of the ubiquitously expressed *Lmbr1* gene, approximately 1 Mb from its target promoter. The exclusive activity of ZRS in the posterior limb bud mesenchyme is critical for normal limb development (Kvon et al. 2016). Elimination of the ZRS causes complete loss of limb-specific *Shh* expression and its mutant embryo shows distally truncated limbs that are indistinguishable from those of *Shh* KO embryos (Sagai et al. 2005). In addition, more than 20 different sites of point mutations in the ZRS associated with limb malformations, such as pre-axial polydactyly, have been reported in multiple species including humans (Hill et al. 2003; Hill and Lettice 2013).

The DNA methylation status of ZRS is correlated with *shh* reactivation during limb regeneration. Contrary to urodele amphibians, anuran amphibians such as *X. laevis* lose their regenerative capability after metamorphosis. The regenerating limb forms a simple spike-shaped structure in *X. laevis* froglet, and also lacks *shh* expression during regeneration (Endo et al. 2000). The ZRS is hypermethylated in the intact limb and blastema of *X. laevis* froglet, whereas it is hypomethylated in those of *X. laevis* tadpole and urodeles (Yakushiji et al. 2007). These results demonstrate that ZRS is gradually methylated in the limb as development progresses, leading to reduced regenerative ability in *X. laevis* froglet. Therefore, reactivation of the *shh* gene through the ZRS is required for complete limb regeneration.

How the ZRS controls the spatiotemporal expression of *Shh* from such a long distance is still not clear; however, a functionally critical sequence of ZRS was identified from a comparison among snakes and other tetrapod genomes (Kvon et al. 2016).

Specifically, a 17-bp sequence is specifically deleted in multiple species of snake but is present in limbed tetrapods and fish. Replacing the endogenous mouse ZRS with that of snake caused complete loss of *Shh* expression and severe limb truncation, which was equivalent to the phenotype caused by deletion of the whole of ZRS. This suggests that, over the course of evolution, snake ZRSs have lost limb enhancer activity. When the 17-bp deleted sequence was inserted into the snake ZRS knock-in mouse, it recovered full enhancer activity and exhibited normal limbs. The 17-bp sequence contains an ETS1 transcription factor binding site; however, loss of the ETS1 site in the 17-bp sequence alone is not sufficient to impair *Shh* expression in limb bud (Lettice et al. 2012). Therefore, uncharacterized transcription factor binding elements are involved in ZRS regulation.

The aim of this study

Reactivation of the developmental gene program is required for proper organ regeneration. To understand how developmental genes are up- or downregulated in a precise spatiotemporal manner, functional assessment of noncoding regulatory elements using regenerative animals is required.

In Chapter I, to develop an effective and simple method of gene disruption in the new model organism, *P. waltl*, for regenerative biology, I targeted several development-related genes using Cas9 RNP and evaluated their efficiency of somatic mutation in these crispants using next-generation sequencing. I found extremely high mutation rates that exceeded 99% for each target locus in the analyzed genes. Moreover, I demonstrated the generation of F_1 offspring from crispants within a year. These results demonstrate the potential to expand this approach to regeneration research.

In Chapter II, using this highly efficient gene knockout method, I targeted the potentially critical site in the limb-specific enhancer of *shh*, and evaluated its function in development and regeneration. Perturbation of the 17-bp snake-specific deletion site decreased the expression of *shh* mRNA and led to severe defects in digit patterning during regeneration. It is noteworthy that this incomplete regeneration was caused by small deletions of ZRS, implying the disruption of a specific transcription factor binding site. Based on these studies, I discuss the function and regulation of the *shh* gene for successful limb regeneration in newt.

CHAPTER Ⅰ

Establishment of a highly efficient gene knockout method in newt using CRISPR-Cas9 ribonucleoprotein complex

Introduction

Recent advances in genome editing using programmable nucleases, such as zinc finger nucleases (ZFNs), transcription activator-like effector nucleases (TALENs) and CRISPR-Cas system, have facilitated reverse genetics in various organisms, including non-model organisms which have the unique biological features. CRISPR-Cas9 needs only two components for gene disruption, an RNA-guided engineered nuclease, Cas9, and a gRNA. gRNA consists of two regions, CRISPR RNA (crRNA) and trans-activating crRNA (tracrRNA). Synthetic gRNA has ~20 nucleotides from the target genome region followed by the sequence 'NGG' referred to as protospacer-adjacent motif (PAM). gRNAs are readily designed and generated as *in vitro*-transcribed single guide RNA (sgRNA) using PCR templates or as chemically synthesized crRNA and tracrRNA.

In amphibians, it was reported that a premixture of recombinant Cas9 protein and gRNA, which forms RNP, quite efficiently introduced mutation in injected founder embryos in *X. tropicalis*. Amplicon sequencing analysis of on-target sites showed that somatic mutation rates reached ~100% in most of injected founder embryos, allowing direct phenotype readouts from them (Sakane et al. 2018). In addition, in urodeles, the effectiveness of CRISPR-Cas has been reported in several studies (Flowers et al. 2014; Fei et al. 2014; Bryant et al. 2017; Elewa et al. 2017).

Urodele amphibian has unique biological properties such as regenerative ability, however, its reverse genetic research has been hampered by difficulties in breeding and long generation time. To overcome this problem, I chose Iberian ribbed newt, *P. waltl,* as an experimental model for regeneration research. *P. waltl* is recently attracting attention as a laboratory newt (Hayashi et al. 2013; Elewa et al. 2017; Urata et al. 2018), because

it can be easily and reaches sexual maturity in 6 months (male) or 9 months (female); in addition, fertilized eggs can be obtained every 2 weeks throughout the year. The genomic sequence of *P. waltl* was obtained and edited using CRISPR-Cas technology, providing a foundation for comparative genomic and regeneration studies (Elewa et al. 2017). However, the efficacy of CRISPR-Cas in *P. waltl* for rapid gene functional analysis has not been well evaluated.

In this chapter, to develop an effective and simple method of gene disruption in *P. waltl* for understanding the molecular mechanism of regeneration, I performed Cas9 RNP injection for gene disruption and demonstrated its feasibility for rapid functional analysis of target genes using crispants.

Materials and Methods

Animals

The Iberian ribbed newts (*P. waltl*) used in this study were maintained in a closed colony following their original purchase from Tao (Chiba, Japan) in 2010. The animals were reared as described previously (Hayashi et al. 2013), unless stated otherwise. The developing stages were defined according to the criteria described by Shi and Boucaut (1995). For anesthesia, MS-222 (Sigma, St. Louis, MO, USA) was used at a final concentration of 0.02%. Animal rearing and treatments were performed and approved in accordance with Guidelines for the Use and Care of Experimental Animals and the Institutional Animal Care and Use Committee of Hiroshima University and Tottori University.

Sequencing of taget genes

The partial genomic sequences and amplicon sequencing data of *tyrosinase (tyr)*, *pax6*, *tbx5* have been deposited in the DDBJ Sequence Read Archive (DRA006550). The cDNA sequence for each gene was predicted from the *P. waltl* transcriptome data set (Elewa et al. 2017) and resequenced (Fig. I-1).

Preparation of gRNAs

All gRNA targeting sequences are highlighted in Fig. I-2. gRNAs were designed using CRISPR-direct (Naito et al. 2015). For sgRNA preparation, templates were assembled by

a PCR-based strategy (Sakane et al. 2017). The oligonucleotide information is listed in Table I-2. DNA templates were purified with a QIAquick PCR Purification Kit (Qiagen, Hilden, Germany); subsequently, sgRNAs were synthesized *in vitro* using a MEGA Shortscript T7 Kit and purified using a MEGA Clear Kit (Thermo Fisher Scientific, Waltham, MA, USA). The synthetic tracrRNA and crRNA were obtained from Integrated DNA Technologies (IDT; Skokie, IA, USA). The tracrRNA and crRNA were annealed in accordance with the manufacturer's instructions just before injection.

Microinjection

Microinjection was performed based on previously reported protocols (Hayashi et al. 2014; Hayashi and Takeuchi 2016; Sakane et al. 2017; Sakane et al. 2018). A brief description of this protocol with minor modification is presented below. The fertilized eggs were treated with 0.5% cysteine in 0.25× Holtfreter's solution for 30 s to remove the jelly. De-jellied eggs were rinsed in 0.25× Holtfreter's solution and transferred into injection medium [4% Ficoll or 0.75% methylcellulose (Sigma) in 0.25× Holtfreter's solution]. The eggshells were removed using forceps and stored at 8°C in injection medium until microinjection. One nanogram of recombinant Cas9 protein (Alt-R *S.p.* Cas9 Nuclease 3NLS; IDT) and 200 pg of sgRNA or 60 pg of crRNA + 160 pg of tracrRNA in 150 mM KCl and 20 mM HEPES buffer were injected into one-cell-stage embryos using Nanoject II (Drummond, Broomall, PA, USA). After microinjection, the embryos were incubated overnight at 25°C in injection medium and then transferred into 0.25× Holtfreter's solution. When injecting Cas9 + sgRNAs, 0.1× Marc's modified Ringer's (MMR) was used instead of 0.25× Holtfreter's solution and 5% Ficoll in 0.3×

MMR was used as injection medium. Phenotypes were evaluated at 6 days postfertilization (dpf) for *tyr* disruption, and 9 dpf for *pax6* and *tbx5* disruption. Embryos that showed developmental defects from 2 dpf were here counted as having developmental defects.

Genotyping

Genomic DNA was extracted from whole bodies of *tyr* (n=5), *pax6* (n=3) using DNeasy Blood and Tissue Kit (Qiagen), individually. Uninjected samples were also collected for each experimental group. An amplicon-sequencing library was prepared based on the Illumina "16S Metagenomic Sequencing Library Preparation." For the first round of PCR, the target regions containing gRNA targeting sites were amplified from individual genomic DNA of uninjected embryos, *tyr* and *pax6* crispants, using KOD FX Neo (TOYOBO, Osaka, Japan) with primer sets containing barcode and overhang adaptor sequences. Each PCR product was purified using a QIAquick PCR Purification Kit (Qiagen) and equal quantities of PCR products were pooled and re-purified using the same kit. For *tbx5* crispants (n=3), the target region was amplified from the tail lysates using KAPA HiFi (Roche Diagnostics, Basel, Switzerland) with primer sets containing overhang adaptor sequences and purified using AMPure XP (Beckman Coulter, Pasadena, CA, USA). Then, each PCR product underwent the second round of PCR using different index primer sets. The second round of PCR was performed to construct a sequence library using a Nextra XT index kit (Illumina, San Diego, CA, USA). The final library was purified and sequenced on Illumina MiSeq. Library construction and sequencing were performed at the National Institute for Basic Biology (NIBB) and Microgen Japan

(Kyoto, Japan). Amplicon-sequencing data were analyzed in accordance with the work of Sakane et al. (2018). PCR and Illumina sequence error rates were determined using uninjected samples, and then mutant reads were counted using an in-house script in R (version 3.3.3; for *tyr* and *pax6*) or CRISPResso (http://crispresso.rocks/; Pinello et al. 2016; for *tbx5*) (Table I-1). For Sanger DNA sequencing of *tyr* F_1 larvae, amplicons were subcloned into pTA2 using Target Clone Plus (TOYOBO). Then, positive clones were selected by colony PCR and sequenced using BigDye Terminator v3.1 Cycle Sequencing kit (Life Technologies, Carlsbad, CA, USA). All primers are listed in Table II-2.

Histological analysis

Embryos were deeply anesthetized with 0.02% MS-222 and fixed with modified Carnoy's solution (65% ethanol, 30% formalin, 5% acetic acid). Tissues were processed for paraffin embedding and then sectioned at 8 μm. Sections were deparaffinized, rehydrated, and stained with hematoxylin and eosin.

Results

Targeted gene disruption of tyr in P. waltl

To examine the efficiency of CRISPR-Cas-mediated gene disruption in *P. waltl*, I first targeted *tyr* (*oculocutaneous albinism IA*) involved in melanin synthesis. Upon the injection of Cas9 RNP as proof of principle, I evaluated two types of guide RNA (gRNA) with the same target sequence prepared in different manners (Fig. I-1–3). One was *in vitro*-transcribed sgRNA using PCR templates and the other was chemically synthesized tracrRNA and crRNA. Surprisingly, a week after the injection of Cas9 RNP, both types of gRNA led to nearly complete loss of pigmentation throughout the body in almost all injected embryos (Fig. I-4A). Furthermore, the same severity of phenotype was observed upon injecting other gRNAs targeting the different coding sequences of *tyr* (Fig. I-5A). Next, to evaluate the efficiency in terms of the somatic mutation rate, amplicon sequencing analysis was performed. Genomic DNA was extracted from the whole body of each crispant (#1–5) and the target genomic locus was amplified and sequenced on a MiSeq platform using a 2× 300-bp paired-end protocol. Even though thousands of reads were analyzed, which may refer to the genotypes of thousands randomly selected cells, almost 100% of alleles were mutated in all analyzed embryos (Fig. I-4B, Table I-1). Amplicon sequencing also revealed that one to three alleles occupied over 99% of total read counts. I also found a low frameshift mutation rate, but severe phenotypes in #2 and #5 embryos, suggesting the functional importance of the target coding region in *tyr* (Fig. I-4B). Dozens of *tyr* crispants were obtained from one experiment; 50 of 70 hatched embryos developed normally and metamorphosed (Fig. I-4C).

It was previously reported that, by breeding *P. waltl* at a warmer temperature (25–26°C), the period required for sexual maturation can be shortened to six months in males and nine months in females (Hayashi et al. 2013). *tyr* crispants also showed sex characteristics within several months and females started to spawn from nine months after fertilization under these rearing conditions. The first F_1 offspring were obtained by crossing crispants with each other within a year (Fig. I-6A). To confirm the genotype of *tyr* F_1 offspring, genomic DNA was extracted from the tail tip and the target site was sequenced. *tyr* alleles were homozygous, with full albino phenotypes being shown in each clutch (Fig. I-6B).

Targeted gene disruption of pax6

For the next proof-of-principle experiment, I targeted *pax6*, which is involved in eye formation (Suzuki et al. 2013; Yasue et al. 2017). Consistent with previous reports, *pax6* crispants showed eye malformations, for example, small eye (class 1), small eye with partial loss of pigmentation (class 2), or no eye (class 3) (Fig. I-7A). Furthermore, all crispants showed eye defects, suggesting the high efficiency of gene disruption by Cas9 RNP, similar to that of *tyr*. The same phenotype was also observed for different sgRNA (Fig. I-5B). Amplicon sequencing analysis revealed that somatic mutation rates were 99% or higher, with a few different types of mutation occurring, similar to the results for *tyr* (Fig. I-7B, Table I-1). I found no relationship between the levels of frame shift mutation rates and the severity of the phenotypes, consistent with a previous report on a mouse study (Yasue et al. 2017).

Targeted gene disruption of tbx5

Finally, I also targeted *tbx5*, which is required for forelimb bud formation (Agarwal et al. 2003; Rallis et al. 2003) and heart development (Bruneau et al. 2001; Garrity et al. 2002). *tbx5* crispants had no detectable forelimb buds consistent with previous reports on other vertebrates (Fig. I-8A). Moreover, hearts of *tbx5* crispants beat slower than those of wild-type embryos without visible blood flow, indicating heart abnormalities. The same phenotype was also observed in the other crRNA:tracrRNA, which targeted a different coding sequence of *tbx5*, but was never seen in the control groups: the uninjected group and the Cas9 protein and tracrRNA-injected (without *tbx5* crRNA) group (Fig. I-8B, Fig. I-5C). Amplicon sequencing analysis revealed virtually complete biallelic disruption in all analyzed embryos with a few different types of mutation (Fig. I-8C).

Discussion

I have presented here a highly efficient and simple method of gene knockout in newt by using Cas9 recombinant protein and synthetic crRNA:tracrRNA duplex or *in vitro*-transcribed sgRNA using PCR-based templates to accelerate reverse genetics in newt (Fig. I-9). Cas9 recombinant protein is more effective than Cas9 mRNA because it can be active immediately after delivery into human cells and zebrafish eggs (Kim et al. 2014; Burger et al. 2016). As previously demonstrated in *Xenopus* (Shigeta et al. 2016; Sakane et al. 2018), Cas9 RNP actually achieved highly efficient gene disruption in *P. waltl*, even in the founder generation. Amplicon sequencing analysis of on-target sites revealed saturating somatic mutations in most of the crispants (> 99%), allowing direct phenotype readouts from them (Ablain et al. 2015; Burger et al. 2016; Zuo et al. 2017; Sakane et al. 2018). For this rapid phenotype analysis, the retention of wild-type and various in-frame alleles is a major concern. In *P. waltl*, I found on average fewer than four mutation alleles in crispants exhibiting severe phenotypes. This suggests that somatic mutations caused by Cas9 RNP resulted in saturation after a few initial cleavages. Sanger sequencing analysis of on-target sites also led to the estimation of a low somatic allele count of genome-edited *P. waltl* (Hayashi et al. 2014; Elewa et al. 2017), and I assume that the longer time for the first cleavage in *P. waltl* (5–6 h at 25°C) would ensure the efficiency of genome editing (Hayashi et al. 2014). Furthermore, I demonstrated the generation of *tyr* F_1 offspring from crispants within a year. Therefore, I am confident that both crispants with saturated mutation and their F_1 progeny will facilitate the functional analysis of genes of interest.

Frameshift mutation disrupts proper translation due to a premature stop codon and nonsense-mediated mRNA decay, so it is the main cause of gene loss of function

caused by CRISPR-Cas. The frameshift rates reached 100% in *tbx5* crispants (Fig. I-8C); however, they were lower in #2 and #5 *tyr* crispants (Fig. I-4B) and #3 *pax6* crispants (Fig. I-6B), even though their phenotypes indicated severe loss of function of the target genes. The gRNAs were designed to recognize exon 1 of *tyr* or DNA binding domain in *pax6*, which would be critical for the function of each protein (Suzuki et al. 2013). Therefore, designing gRNAs against the functional domains would contribute to efficient gene loss of function, even if in-frame mutations occur (Burger et al. 2016; Shigeta et al. 2016). I found phenotypic spectrum in *pax6* crispants, as with the previous reports in mouse and *Xenopus* (Suzuki et al. 2013; Yasue et al. 2017). *pax6* is a transcription factor that regulates itself during eye formation. Therefore, its somatic mutation (e.g., various truncated proteins and mosaicism in optic cup and lens placode) may perturb the *pax6* gene network and result in varying degrees of eye malformation. In addition, designing multiple gRNAs to the target gene is also preferable for efficient gene disruption, since it is known that the cleavage activity of programmable nucleases is affected by the chromatin state at the target site (Wu et al. 2014; Kuscu et al. 2014). Actually, phenotype frequencies were shown to vary in a manner dependent on the sequences of gRNAs against a target gene. In my study, at least one gRNA induced a severe phenotype in ~80% of embryos when I tested two or three gRNAs against each target gene. Moreover, confirming the identical phenotype using multiple gRNAs is one way of avoiding the misreading of phenotypes and obtaining reliable phenotypes due to off-target effects in salamanders, in view of their huge genome size (Fei et al. 2014). Recently, the genome of *P. waltl* has been sequenced (Elewa et al. 2017), so more detailed off-target evaluation can now be applied; for example, candidates of off-target sites can be identified from genome sequence data and unexpected mutations are easily examined by performing a

heteroduplex mobility assay on the candidates (Zhu et al. 2014; Shigeta et al. 2016).

>tyr

```
cg atg ATG GTG TGG GGC CTG GCC GTT TGT GTG CTG CTG TGG GCT CTG CCC
       M  V  W  G  L  A  V  C  V  L  L  W  A  L  P
TGT CAG GCC CAG TTC CCG CGC CCC TGC GCC TCC TCC GCG GCT CTA CTC AG
 C  Q  A  Q  F  P  R  P  C  A  S  S  A  A  L  L  S
C AAG GAG TGC TGT CCG GTG TGG GAT GGC GAT GGC TCT CCC TGT GGC CAG C
   K  E  C  C  P  V  W  D  G  D  G  S  P  C  G  Q  L
TC TCT GGC CGG GGC AGC TGC CAG GCC GTG GAG GTG TCA CAG GCC CCC AAC
    S  G  R  G  S  C  Q  A  V  E  V  S  Q  A  P  N
GGA CCC CAG TTT CCG TTT TCA GGT GTG GAT GAC AGG GAG GAT TGG CCC AT
 G  P  Q  F  P  F  S  G  V  D  D  R  E  D  W  P  I
C GTC TTC TAC AAC CGC ACC TGC CGC TGC GTG CCG CCC TTC GGC GGC TTC C
   V  F  Y  N  R  T  C  R  C  V  P  P  F  G  G  F  Q
AG TGC GGG GAT TGC GCC TTC GGG CGT TGG GGT CCG GAG TGC GCG GAC AAG
    C  G  D  C  A  F  G  R  W  G  P  E  C  A  D  K
CGC TTG CAG GTG CGC AAG AGC ATC CTT CAG CTC AGT GCC ACC GAG AGC GC
 R  L  Q  V  R  K  S  I  L  Q  L  S  A  T  E  S  A
T CGA CTC CTG GCC TAT CTG AAC CTG GCC AAG CGC ACC ATC AGC CCC GAC T
   R  L  L  A  Y  L  N  L  A  K  R  T  I  S  P  D  F
TC GTG ATC GCC ACT GGG ACC TAC GAG CAG ATG GAC AAC GGG TCC CGG CCG
    V  I  A  T  G  T  Y  E  Q  M  D  N  G  S  R  P
CTC TTC GCC GAC ATC AGC GTC TAC GAC CTC TTT GTG TGG ATT CAC TAC TA
 L  F  A  D  I  S  V  Y  D  L  F  V  W  I  H  Y  Y
T GCG TCA CGG GAC ACC TGG GTG CCG GCG GAG GGC GAG GAG GAC ACA GCT G
   A  S  R  D  T  W  V  P  A  E  G  E  E  D  T  A  V
TG TGG CGT AAC ATC GAC TTC GCA CAC GAG GCG CCC GCC TTC CTG CCG TGG
    W  R  N  I  D  F  A  H  E  A  P  A  F  L  P  W
CAC CGG ATC TAC CTG CTC CTC TGG GAA CGC GAG CTC CAG AAG GTG ACC GG
 H  R  I  Y  L  L  L  W  E  R  E  L  Q  K  V  T  G
A GAT GAG AAC TTC ACC ATC CCG TAC TGG GAC TGG AGG GAC GCC CAG GGC T
   D  E  N  F  T  I  P  Y  W  D  W  R  D  A  Q  G  C
GT GAC GTC TGC ATC GAC CAG CTG ATG GGG GAC CGG CAC CCG ACA GTA CCC
    D  V  C  I  D  Q  L  M  G  D  R  H  P  T  V  P
GGC CTG CTA AGC CCG GCT TCA TTC TTC TCC TCC TGG CAG GTC ATT TGC AG
 G  L  L  S  P  A  S  F  F  S  S  W  Q  V  I  C  S
C AAG GCT GAA GAG TAT AAC AAT CTA CGC ATT CTA TGC AAT GGT ACA CAA G
   K  A  E  E  Y  N  N  L  R  I  L  C  N  G  I  Q  E
AA GGA CCT TTA GTC CGG AAC CCT GGA AAT CAC GAT AAA AGC AGG GTT CAG
    G  P  L  V  R  N  P  G  N  H  D  K  S  R  V  Q
AGG CTC CCA ACT TCA GAG GAG GTG GAG TTC TGT GTA AGC CTT ACA CAG TA
 R  L  P  T  S  E  E  V  E  F  C  V  S  L  T  Q  Y
T GAT ACA GAG CCG ATG GAC AGG TCA GCT AAC CTG AGC TTC AGA AAC ACA T
   D  T  E  P  M  D  R  S  A  N  L  S  F  R  N  T  L
TG GAA GGA TTT GCC AAT CCA AGC ACA GGA ATT GCA AAC CGA TCA ATA AGT
    E  G  F  A  N  P  S  T  G  I  A  N  R  S  I  S
GCT TTA CAT AAT TCT CTC CAT GTG TTT ATG AAT GGC TCC ATG TCA TCG GT
 A  L  H  N  S  L  H  V  F  M  N  G  S  M  S  S  V
T CAA GGG TCG GCC AAT GAC CCC ATT TTT GTA ATT CAT CAT GCC TTT GTT G
   Q  G  S  A  N  D  P  I  F  V  I  H  H  A  F  V  D
AT AGC ATA TTC GAG CAA TGG CTT AGA AGA CAC CAA CCA TTA TTA GAT GTT
    S  I  F  E  Q  W  L  R  R  H  Q  P  L  L  D  V
TAT CCA GAA GCG AGT GCG CCC ATT GGG CAC AAT CGG GAA TAC TTC ATG GT
 Y  P  E  A  S  A  P  I  G  H  N  R  E  Y  F  M  V
C CCC TTC CTT CCA CTG GCC ACA AAT GGT GAA TTT TTC CTC CCA TCA AGA G
   P  F  L  P  L  A  T  N  G  E  F  F  L  P  S  R  D
AC CTG GGC TAT GAA TAT GAA TAT TTA GTA GAA CCA GCT CCT GGC ACC TTT
    L  G  Y  E  Y  E  Y  L  V  E  P  A  P  G  T  F
CAA GAT TTT CTG GAA CCC TAC CTT GAA CAA GCC AGT CGG ATA TGG CAG TG
 Q  D  F  L  E  P  Y  L  E  Q  A  S  R  I  W  Q  W
G CTT GTG GCA GCC GCC TTG CTT GGT GGT GTG ATT ACT GCG GTG ATT GCA A
   L  V  A  A  A  L  L  G  G  V  I  T  A  V  I  A  S
GC CTT GTC ACT CTT GCC TGT CGG AAG CGG AAG CGA CGA AGC AAC CCG GAA
    L  V  T  L  A  C  R  K  R  K  R  R  S  N  P  E
GAG AGG CAG CCC TTA CTC ATG GAG GCA GAG GAC TAC CAA AGC ACT TAT CA
 E  R  Q  P  L  L  M  E  A  E  D  Y  Q  S  T  Y  Q
A TCA CAG TTG TAG tag acg aca aca atc tga cat tga aaa gga tta aat a
   S  Q  L  *
catcaagtgtatggaatgtaaatggagggcttgctcccatatatatacga
ctaactttctttcagatgacgcagcagcattattgtggcctatttgacag
caggtttttaaaagtgtcctcgttcccggatttttacacattcgtgtgta
gaagattacattgaatagcaaccaacttttattattatttcttctgtctc
cctaatatatcttagctaaacctaatgtgcatggaacaaaatattttat
aaaagccttaggctttttcttagctgacctgctgccttgtatgcatcatct
gctgtgatgcacatctgtaaactgttggttggtgtgccttaaaaaaaac
atgcccattgggtattcaaataaaaaggcatggat

>pax6

aggcgaaatagctccctgattagtgtccctttcggagccgaggcattaga
cactgctaatcccagcggcggctaattgagcgcttgtagaaataatatat
gagatttcttctcctttgcccggagaacatatcaaagttttttttcccacc
ttttcttttgctcttctataagcggacgggtgtaaaaaaagctccttttg
atttccatgttgcaaaggacttggctttttttcctgctgaaagggaccat
cgttgaatgtattccgtctcctgcaaaattgcttctgtactcaaggaact
ttcttcaaatacacggagattattttggccttttatcatttaaaaaaaa
caaggaaccaggcggcgttgggttttttcgtgaaaagttgtggagctgtt
ttggggaagaaggcgcctgtcgcttggagcgcggagggcacagagcactg
aggcgaggtagccagcgtgtgtcattgcacagcgaggagctaacgaccgg
cagcggagaggggccgaatctgagcaccgcagaccggcagccatgagga
gggaagactttaagtagaggcaagcagatgtgtgagccctttaattgcat
gacaagacagccaccccacatttcaggactacataagggagacacaaggg
```

att gcg ctg gag cag ttc aac ATG CAG AAC AGT CAT AGC GGA GTC AAC CA

```
                                M  Q  N  S  H  S  G  V  N  Q
 G CTC GGG GGA GTG TTC GTG AAC GGC AGA CCC CTG CCC GAC TCC ACC CGC C
    L  G  G  V  F  V  N  G  R  P  L  P  D  S  T  R  Q
AG AAG ATC GTG GAG CTC GCC CAC AGC GGA GCC CGG CCC TGC GAC ATC TCC
    K  I  V  E  L  A  H  S  G  A  R  P  C  D  I  S
CGC ATC CTG CAG ACC CAT GCA GAT GCA AAA GTC CAA GTG CTG GAC AGT CA
 R  I  L  Q  T  H  A  D  A  K  V  Q  V  L  D  S  Q
A AAC GTG TCC AAT GGT TGT GTG AGT AAG ATT CTG GGC AGG TAT TAC GAG A
   N  V  S  N  G  C  V  S  K  I  L  G  R  Y  Y  E  T
CG GGT TCC ATC CGG CCG CGC GCC ATC GGA GGC AGC AAG CCC AGG GTG GCG
    G  S  I  R  P  R  A  I  G  G  S  K  P  R  V  A
ACC CCC GAG GTG GTC AGC AAG ATC GCG CAG TAC AAG CGG GAG TGC CCG TC
 T  P  E  V  V  S  K  I  A  Q  Y  K  R  E  C  P  S
C ATC TTC GCC TGG GAG ATC CGC GAC CGG CTG CTG TCT GAG GGG GTC TGC A
   I  F  A  W  E  I  R  D  R  L  L  S  E  G  V  C  T
CC AAC GAC AAC ATC CCC AGC GTG TCA TCG ATA AAC CGA GTG CTC CGC AAC
    N  D  N  I  P  S  V  S  S  I  N  R  V  L  R  N
CTG GCT AGC GAA AAG CAA CAA ATG GGC GCA GAC GGA ATG TAC GAC AAG CT
 L  A  S  E  K  Q  Q  M  G  A  D  G  M  Y  D  K  L
G CGG ATG CTG AAC GGA CAG ACG GGC ACC TGG GGC ACG CGG CCG GGC TGG T
   R  M  L  N  G  Q  T  G  T  W  G  T  R  P  G  W  Y
AC CCG GGG ACC TCG GTG CCG GGG CAG CCC ACA CCA GAT GGC TGC CAA CAA
    P  G  T  S  V  P  G  Q  P  T  P  D  G  C  Q  Q
CAG GAA GGG GGA GGC GAG AAC ACC AAC TCC ATC AGC TCG AAC GGA GAA GA
 Q  E  G  G  G  E  N  T  N  S  I  S  S  N  G  E  D
C TCC GAC GAG GCC CAG ATG AGG CTG CAG CTG AAA CGC AAA CTG CAA AGG A
   S  D  E  A  Q  M  R  L  Q  L  K  R  K  L  Q  R  N
AC AGG ACG TCT TTC ACT CAG GAG CAG ATC GAG GCT CTG GAG AAA GAG TTT
    R  T  S  F  T  Q  E  Q  I  E  A  L  E  K  E  F
GAA CGA ACA CAI IAC CCI GAC GIG III GCA AGA GAG AGA CIA GCI GCC AA
 E  R  T  H  Y  P  D  V  F  A  R  E  R  L  A  A  K
A ATA GAC CTA CCT GAA GCA CGA ATA CAG GTC TGG TTT TCA AAC AGG AGG G
   I  D  L  P  E  A  R  I  Q  V  W  F  S  N  R  R  A
CA AAG TGG CGA AGG GAA GAG AAA CTG CGG AAC CAG AGG AGG CAA GCA AGC
    K  W  R  R  E  E  K  L  R  N  Q  R  R  Q  A  S
AAC ACT CCC AGC CAT ATC CCC ATC AGG AGC AGC TTC AGC ACT AGT GTG TA
 N  T  P  S  H  I  P  I  S  S  S  F  S  T  S  V  Y
C CAG CCC ATC CCC CAG CCC ACA ACA CCC GTT TCA TTT ACA TCC GGG TCC A
   Q  P  I  P  Q  P  T  T  P  V  S  F  T  S  G  S  M
TG TTG GGC AGA ACA GAC ACA TCC CTG ACA AAC ACA TAC GGC GGC CTA CCA
    L  G  R  T  D  T  S  L  T  N  T  Y  G  G  L  P
CCC ATG CCC AGC TTC ACA ATG GGC AAC AAC CTG CCT ATG CAA CCC CCA GT
 P  M  P  S  F  T  M  G  N  N  L  P  M  Q  P  P  V
T CCC AGC CAG GCC TCC TCC TAC TCT TGC ATG CTG CCC TCT AGT CCG TCA G
   P  S  Q  A  S  S  Y  S  C  M  L  P  S  S  P  S  V
TG AAT GGG CGG AGC TAT GAT ACA TAC ACA CCT CCT CAC ATG CAG GCA CAC
    N  G  R  S  Y  D  T  Y  T  P  P  H  M  Q  A  H
ATG AAC AGC CAG TCC ATG GGC ACA GCT GGC GCC ACT TCG ACA GGT CTC AT
 M  N  S  Q  S  M  G  T  A  G  A  T  S  T  G  L  I
T TCC CCT GGA GTG TCA GTC CCA GTA CAA GTT CCC GGC AGT GAA CCT GAC C
   S  P  G  V  S  V  P  V  Q  V  P  G  S  E  P  D  L
TG TCT CAA TAC TGG CCA AGA TTA CAG TAA aaa ccg ggc taa cat agc caa
    S  Q  Y  W  P  R  L  Q  *
tgactttgtggagaacagttggatgttcagcagtattctatagaggaggg
acacggctggcaaaaaagtatccctcccctgcaactctgccctgagttgg
gaggcttcggaaagacttttcaaggggacctttgcacaatttgaaggcgt
tatatcagttggaacaaatcttcatttttggtatacaaccctttactcatt
ttgtgtgctacttgtaaatgggcatttgtatgttataagacaagaacaac
ccaaactgactggacggacggtatttggcctaagctgatcattacgtttt
ttttttaacaaaaaaaaaaaatggaagccatgatggaccagcctttgccac
gatttccagagttttcgtcgacaaatacccggacaggtctaccgcgttgtg
cataagcagactggcgttccatgttttttttctatcattccactgcatata
aactgaaactggaaggtgtaggtaaagacaatgaagccaatggaaattcc
aaaggcgaaaagcaatccagatgatgtttatgtctacagacccgggtaaag
agaaaacttcgagaaggaagaaacaagtttggtagataacatttaaaaaa
taaggtagattgtgtcttcgatataatccgatttgtttttatgtcgaaatg
taagtatttgtcttccctagaaatctcccggaatgatttctatataaaag
ttaatttcatttatatttgacaagaatattctatagatgttttatacaca
ttttccatgcatcttgcgtttctttctttttgggggggaggggagttcag
cgaagagtttattgttcctacctgtagctgtactacatgttcacaagtca
gatcatctttgtgcatctagaactcattcctaatcaattaaaagtgcttg
caagagttttcaatttaagtgttttgaagttgttcacagcgacatatcaa
acgtaaccattgttgattgtaaaaaccatgccaaagccttttgtatttcct
ttattatactatttttttta
```

Figure I-1. partial cDNA sequences of target genes with deduced amino acid sequences
Capital letters indicate predicted open reading frames.

>tyr_partial_genome_sequence

tagcgtgcccattcacccggcacataacttttttcccgagacggccctttc
catgcaggccggtcatgtgcgcaaagacgcaggctcgcttataatgctgc
ttttatgttcacgcgctggcggggcatccgcacggtggtgtgtacacgtg
gttccgatgtgatatccgggggtggcgggtcggagggtgtgtgtatgtga
ccttactggggtgttgcaggttagctcactcttcacaaagcaCGATGATG
GTGTGGGGCCTGGCCGTTTGTGTGCTGCTGTGGGCTCTGCCCTGTCAGGC
CCAGTTCCCGCGCCCCTGCGCCTCCTCCGCGGCTCTACTCAGCAAGGAGT
GCTGTCCGGTGTGGGATGGCGATGGCTCTCCCTGTGGCCAGCTCTCTGGC
CGGGGCAGCTGCCAGGCCGTGGAGGTGTCACAGGCCCCCAACGGACCCCA
GTTTCCGTTTTCAGGTGTGGATGACAGGGAGGATTGGCCCATCGTCTTCT
ACAACCGCACCTGCCGCTGCGTGCCGCCCTTCGGCGGCTTCCAGTGCGGG
GATTGCGCCTTCGGGCGTTGGGGTCCGGAGTGCGCGGACAAGCGCTTGCA
GGTGCGCAAGAGCATCCTTCAGCTCAGTGCCACCGAGAGCGCTCGACTCC
TGGCCTATCTGAACCTGGCCAAGCGCACCATCAGCCCCGACTTCGTGATC
GCCACTGGGACCTACGAGCAGAT

tyr gRNA (Fig. 1): CCGAGAGCGCTCGACTCCTGGCC
tyr gRNA2 (Fig. S4): GGCCGTTTGTGTGCTGCTGTGGG
tyr gRNA3 (Fig. S4): CCTGGCCAAGCGCACCATCAGCC

>pax6_partial_genome_sequence

GAGTGTTCGTGAACGGCAGACCCCTGCCCGACTCCACCCGCCAGAAGATC
GTGGAGCTCGCCCACAGCGGAGCCCGGCCCTGCGACATCTCCCGCATCCT
GCAGgtgaacaggcgggccagcctcccggccgctcccggagcgctcccgc
ggtgatgcactttagcacacgaactcgcgcaccgctcggtccagctcctt
taaagacgcatttcacctgcttaatttaaaggccaatttcatctgcttgc
ggctttgtgcttgttatgcttgtagtttattttaaaaaatcacttttttt
agttatttaaacatatactatgtaaatatatattgtatacacattaattg
tcatggcctgtcaagtagaaatggcagtctcgcctatgatttatgcacac
ttaagtccagctgtttttttaagccgatttttatttgtagggacatattgta
aatttaaacattttggcttattttagagctgttttctacatttagtattt
cagtatttttatatggcaaaaccaaatatatgtctagttttgcatattta
ctgtacaggtataatgctacaataatattgacagagtagcgccctgtaat
gtgtttaacgcatcacacatatctatatctatacatagctgtagggccac
aaatgtacatttaagaaaacttttaagtaagttctcataccatttaaggt
atatttttgtattatAGACCCATGCAGATGCAAAAGTCCAAGTGCTGGAC
AGTCAAAACGTaagcctgtcattgtttatgcctacttaaaacattttacc
attgtcttgaaattattaataatgtgattttctgtcccttcccctgatca
gGTGTCCAATGGTTGTGTGAGTAAGATTCTGGGCAGGTATTACGAGACGG
GTTCCATCCGGCCGCGCGCCATCGGAGGCAGCAAGCC

pax6 gRNA (Fig. 3): CCGACTCCACCCGCCAGAAGATC
pax6 gRNA2 (Fig. S4): CCGGCCCTGCGACATCTCCCGCA

>tbx5_partial_genome_sequence_1

ctacaacaatgattgtcccacgagccactgcctatcgttattttattatt
gtgcaaaaagctcctaatctaaatctctggagctgagggagtggaatggc
ctagccgtaataaagccaaaagtgtattaattgaaacaaagaatgcacgg
gcagaaaacaattgtaggacccaatcctagcaccacagacgacagtcatg
ccatgctacacacgtgtaagcatgtgcgagacagaaagcgagagctcgac
tgcagttttcgcactctcatgcatgtctacagcaacctaaattgttcctt
tgtttaCAGGGCATGGAAGGAATTAAGGTGTTTTTACATGRGCGAGAACT
GTGGCTAAAATTCCATGACGTGGGGACAGAGATGATCATCACAAAGGCTG
GAAGGtaaacaatatttgtacatacatgttta

>tbx5_partial_genome_sequence_2

AAGACCGAGTGGGGGGAGCCGGCGCCATGACGGACTCGGACGAGGGCTTT
GGGATGCCGGACACCCCAGTGGACCCAGAGTCCAAGGAGCTGCAGTCTGA
CTCCAAGCCGGACAGCCAGCTCGGCGCGGGAAGCAAGCCCCCCTCCTCTC
CCCAGGCCGCCTTCACCCAGCAG

tbx5 gRNA (Fig. 4): CCATGACGTGGGGACAGAGATGA
tbx5 gRNA2 (Fig. S4): GGACGAGGGCTTTGGGATGCCGG

Figure I-2. partial genome sequences of target loci
Capital letters are the sequences found in partial cDNA sequences. Red letter indicates predicted start codon. gRNA target protospacer and PAM sequence are marked in gray and red, respectively. Underline indicates primer sequence for amplicon-seq.

	frog	chick	mouse	human
tyr	NP_001096518.1	P55024	P11344	P14679
pax6	F6SK62	F1NF66	P63015	P26367
tbx5	Q3SA47	Q9PWE8	P70326	Q99593

```
>tyr
human           -----MLLAVLYCLLWSFQTSAGHFPRACVSSKNLMEKECCPPWSGDRSPCGQLSGRGSCQ
Mouse           -----MFLAVLYCLLWSFQISDGHFPRACASSKNLLAKECCPPWMGDGSPCGQLSGRGSCQ
Chick           -----MFLFAMGLLLVILQPSTGQFPRVCANTQSLLRKECCPPWDGDGTPCGERSNRGTCQ
Frog            MERNMVPLAFCCLFFFLHVCRGQFPRACSTAESLLSKECCPVWSGDGSSCGQLSGRGVCQ
Newt            -----MVWGLAVCVLLWALPCQAQFPRPCASSAALLSKECCPVWDGDGSPCGQLSGRGSCQ
                    *.       ::     . .:*** * .:  *: ***** * ** :.**: *.** **

human           NILLSNAPLGPQFPFTGVDDRESWPSVFYNRTCQCSGNFMGFNCGNCKFGFWGPNCTERR
Mouse           DILLSSAPSGPQFPFKGVDDRESWPSVFYNRTCQCSGNFMGFNCGNCKFGFGGPNCTEKR
Chick           RILLSQAPLGPQFPFSGVDDREDWPSVFYNRTCRCRGNFMGFNCGECKFGFSGQNCTERR
Frog            DVVLTSSATGPQFPFTGVDDRENWPTVFYNRTCQCLGNFMGYNCADCKFGFRGPNCTERR
Newt            AVEVSQAPNGPQFPFSGVDDREDWPIVFYNRTCRCVPPFGGFQCGDCAFGRWGPECADKR
                 : ::.:. ******.*******.** ********:*   * *:::*.:* **  * :*:::*

human           LLVRRNIFDLSAPEKDKFFAYLTLAKHTISSDYVIPIGTYGQMKNGSTPMFNDINIYDLF
Mouse           VLIRRNIFDLSVSEKNKFFSYLTLAKHTISSVYVIPTGTYGQMNNGSTPMFNDINIYDLF
Chick           LRTRRNIFQLTISEKDKFLAYLNLAKNIPSKDYVIATGTYAQMNNGSNPMFRNINVYDLF
Frog            TMIRKEIFRMSSAEKSKFVAYLNLAKHTTSRDYVIVTGTYAQMNNGSNPMFADINVYDLF
Newt            LQVRKSILQLSATESARLLAYLNLAKRTISPDFVIATGTYEQMDNGSRPLFADISVYDLF
                   *:.*: :: .*. ::.:**.***.  *  :**  *** **.*** *:* :*.:****

human           VWMHYYVSMDALLGGS------EIWRDIDFAHEAPAFLPWHRLFLLRWEQEIQKLTGDENF
Mouse           VWMHYYVSRDTLLGGS------EIWRDIDFAHEAPGFLPWHRLFLLLWEQEIRELTGDENF
Chick           VWMHYYASRDTLLGGS------NVWRDIDFAHEAPGFLPWHRAFLLLWEREIQKITGDENF
Frog            VWMHYYASRDVFIGED------ALWRDIDFAHEAPAFVPWHRYFLLHWEHEIQKLTGDENF
Newt            VWIHYYASRDTWVPAEGEEDTAVWRNIDFAHEAPAFLPWHRIYLLLWERELQKVTGDENF
                **:***.* *. :  .       :**:********.*:**** :** **:*:::******

human           TIPYWDWRDAEKCDICTDEYMGGQHPTNPNLLSPASFFSSWQIVCSRLEEYNSHQSLCNG
Mouse           TVPYWDWRDAENCDICTDEYLGGRHPENPNLLSPASFFSSWQIICSRSEEYNSHQVLCDG
Chick           TIPYWDWRDAEDCVICTDEYMGGQHPTNPNLLSPASFFSSWQVICTQSEEYNSQQALCNA
Frog            TIPFWDWRDAQGCDICTDELLGGVHPTTTSLLSPASFFASWQIVCSRPEEYNAQRILCNG
Newt            TIPYWDWRDAQGCDVCIDQLMGDRHPTVPGLLSPASFFSSWQVICSKAEEYNNLRILCNG
                *:*:******: * :* *: :*. **  ..********:***::*:: ****  : **:.

human           TPEGPLRRNPGNHDKSRTPRLPSSADVEFCLSLTQYESGSMDKAANFSFRNTLEGFASPL
Mouse           TPEGPLLRNPGNHDKAKTPRLPSSADVEFCLSLTQYESGSMDRTANFSFRNTLEGFASPL
Chick           TSEGPILRNPGNNDKSRTPRLPSSSEVEFCLTLTQYESGSMDKMANYSFRNTLEGFADPH
Frog            TGEGPLFRNPGGHDRSRTPRLPTTAEVELCLSLTNYETEPMDRSANFSFRNTLEGFADPR
Newt            TQEGPLVRNPGNHDKSRVQRLPTSEEVEFCVSLTQYDTEPMDRSANLSFRNTLEGFANPS
                * ***: ****.:*:::. ***:: :**:*::**:*:: .**: ** **********.*

human           TGIADASQSSMHNALHIYMNGTMSQVQGSANDPIFLLHHAFVDSIFEQWLRRHRPLQEVY
Mouse           TGIADPSQSSMHNALHIFMNGTMSQVQGSANDPIFLLHHAFVDSIFEQWLRRHRPLLEVY
Chick           TAISNISQSGLHNALHIYMNGSMSQVQGSANDPIFILHHAFVDSIFERWLRRHRPMLEVY
Frog            TGIANRSQSNMHNSLHVFLNGSMSSVQGSANDPVFVLHHAFVDSIFEQWLRRHGASVDIY
Newt            TGIANRSISALHNSLHVFMNGSMSSVQGSANDPIFVIHHAFVDSIFEQWLRRHQPLLDVY
                *.*:: * * :**:**:::**:**.********:*::**********:***** .  ::*

human           PEANAPIGHNRESYMVPFIPLYRNGDFFISSKDLGYDYSYLQDSDPDSFQDYIKSYLEQA
Mouse           PEANAPIGHNRDSYMVPFIPLYRNGDFFITSKDLGYDYSYLQESDPGFYRNYIEPYLEQA
Chick           PAANAPIGHNRENYMVPFIPLYRNGEFFISSRELGYDYEYLQEPALGSFQDFLIPYLKQA
Frog            PEANAPIGHNRGYYMVPFIPLYTNGEFFAASRDLGYDYDYLAES--GSIEDFLLPYLEQA
Newt            PEASAPIGHNREYFMVPFLPLATNGEFFLPSRDLGYEYEYLVEPAPGTFQDFLEPYLEQA
                * *.*******  :****:**  **:** .*::***:*.** :.  .  .::: .**:**

human           SRIWSWLLGAAMVGAVLTALLAGLVSLLCRHKRK---QLPEEKQPLLMEKEDYHSLYQSH
Mouse           SRIWPWLLGAALVGAVIAAALSGLSSRLCLQKKKKKKQPQEERQPLLMDKDDYHSLLYQS
Chick           HQIWPWLVGAAVIGGIITAVLSGLILACRKKRKG----TSPEIQPLLTESEDYNNVSYQS
Frog            RQIWQWLVGAAVVGGLITAVIATIVGLACRRKRK---FPSEETQPLLMEAEDYQPTYQSH
Newt            SRIWQWLVAAALLGGVITAVIASLVTLACRKRKR--RSNPEERQPLLMEAEDYQSTYQSQ
                 :** **:.**::*.:::* :: :      :::        * **** : :**:    .

human           L-
Mouse           HL
Chick           HF
Frog            L-
Newt            L-
```

```
>pax6
Mouse           ------------------------------------------------------------
Chick           MCEPPRCRRGQRARLPGKWPLPDASPRRASRPEALCAPQPSPRPGDTPRGARRSRLTRVS
Human           ------------------------------------------------------------
Newt            ------------------------------------------------------------
Frog            ------------------------------------------------------------


Mouse           ------------------MQNSHSGVNQLGGVFVNGRPLPDSTRQKIVELAHSGARPCDI
Chick           LPQTAPGEPRGTPLPRPTMQNSHSGVNQLGGVFVNGRPLPDSTRQKIVELAHSGARPCDI
Human           ------------------MQNSHSGVNQLGGVFVNGRPLPDSTRQKIVELAHSGARPCDI
Newt            ------------------MQNSHSGVNQLGGVFVNGRPLPDSTRQKIVELAHSGARPCDI
Frog            ------------------MSLGHSGVNQLGGVFVNGRPLPDSTRQKIVELAHSGARPCDI
                                   *. .****************************************


Mouse           S---RILQ--------------VSNGCVSKILGRYYETGSIRPRAIGGSKPRVATPEVVS
Chick           S---RILQ--------------VSNGCVSKILGRYYETGSIRPRAIGGSKPRVATPEVVS
Human           S---RILQ--------------VSNGCVSKILGRYYETGSIRPRAIGGSKPRVATPEVVS
Newt            S---RILQTHADAKVQVLDSQNVSNGCVSKILGRYYETGSIRPRAIGGSKPRVATPEVVS
Frog            SRILQ-----------------VSNGCVSKILGRYYETGSIRPRAIGGSKPRVATPEVVS
                *   :                 ************************************


Mouse           KIAQYKRECPSIFAWEIRDRLLSEGVCTNDNIPSVSSINRVLRNLASEKQQMGADGMYDK
Chick           KIAQYKRECPSIFAWEIRDRLLSEGVCTNDNIPSVSSINRVLRNLASEKQQMGADGMYDK
Human           KIAQYKRECPSIFAWEIRDRLLSEGVCTNDNIPSVSSINRVLRNLASEKQQMGADGMYDK
Newt            KIAQYKRECPSIFAWEIRDRLLSEGVCTNDNIPSVSSINRVLRNLASEKQQMGADGMYDK
Frog            KIAQYKRECPSIFAWEIRDRLLSEGVCTNDNIPSVSSINRVLRNLASEKQQMGADGMYDK
                ************************************************************


Mouse           LRMLNGQTGSWGTRPGWYPGTSVPGQPTQDGCQQQEGGG--ENTNSISSNGEDSDEAQMR
Chick           LRMLNGQTGTWGTRPGWYPGTSVPGQPAQDGCPQQEGGG--ENTNSISSNGEDSDEAQMR
Human           LRMLNGQTGSWGTRPGWYPGTSVPGQPTQDGCQQQEGGG--ENTNSISSNGEDSDEAQMR
Newt            LRMLNGQTGTWGTRPGWYPGTSVPGQPTPDGCQQQEGGG--ENTNSISSNGEDSDEAQMR
Frog            LRMLNGQTGTWGTRPGWYPGTSVPGQPAQDGCQPQEGGGGGENTNSISSNGEDSDEAQMR
                *********:*****************: ***  *****  ********************


Mouse           LQLKRKLQRNRTSFTQEQIEALEKEFERTHYPDVFARERLAAKIDLPEARIQVWFSNRRA
Chick           LQLKRKLQRNRTSFTQEQIEALEKEFERTHYPDVFARERLAAKIDLPEARIQVWFSNRRA
Human           LQLKRKLQRNRTSFTQEQIEALEKEFERTHYPDVFARERLAAKIDLPEARIQVWFSNRRA
Newt            LQLKRKLQRNRTSFTQEQIEALEKEFERTHYPDVFARERLAAKIDLPEARIQVWFSNRRA
Frog            LQLKRKLQRNRTSFTQEQIEALEKEFERTHYPDVFARERLAAKIDLPEARIQVWFSNRRA
                ************************************************************


Mouse           KWRREEKLRNQRRQASNTPSHIPISSSFSTSVYQPIPQPTTPVSSFTSGSMLGRTDTALT
Chick           KWRREEKLRNQRRQASNTPSHIPISSSFSTSVYQPIPQPTTPG------SMLGRTDTALT
Human           KWRREEKLRNQRRQASNTPSHIPISSSFSTSVYQPIPQPTTPVSSFTSGSMLGRTDTALT
Newt            KWRREEKLRNQRRQASNTPSHIPISSSFSTSVYQPIPQPTTPVS-FTSGSMLGRTDTSLT
Frog            KWRREEKLRNQRRQASNTPSHIPISSSFSTSVYQPIPQPTTPVSSFTSGSMLGRTDTALT
                ******************************************       ********:**


Mouse           NTYSALPPMPSFTMANNLPMQPPVPSQTSSYSCMLPT----SPSVNGRSYDTYTPPHMQT
Chick           NTYSALPPMPSFTMANNLPMQPPVPSQTSSYSCMLPT----SPSVNGRSYDTYTPPHMQT
Human           NTYSALPPMPSFTMANNLPMQPPVPSQTSSYSCMLPT----SPSVNGRSYDTYTPPHMQT
Newt            NTYGGLPPMPSFTMGNNLPMQPPVPSQASSYSCMLPS----SPSVNGRSYDTYTPPHMQA
Frog            NSYSALPPMPSFTMGNNLPMQPPPPPTHTHTYLFLSSNAMCPNTTTYDPYGPFIRNPRHR
                *:*..*********.******** *.  :    :*.:    . :..  .*..:     :


Mouse           HMNSQPMGTSGTTSTGLISPGVSVPVQVPGSEPDMSQYWPRLQ
Chick           HMNSQPMGTSGTTSTGLISPGVSVPVQVPGSEPDMSQYWPRLQ
Human           HMNSQPMGTSGTTSTGLISPGVSVPVQVPGSEPDMSQYWPRLQ
Newt            HMNSQSMGTAGATSTGLISPGVSVPVQVPGSEPDLSQYWPRLQ
Frog            HGNCQPQSSKGTNLKCLISPGVSVPVQVPGSEPDMSQYWPRLQ
                * *.*. .: *:. . ******************:********
```

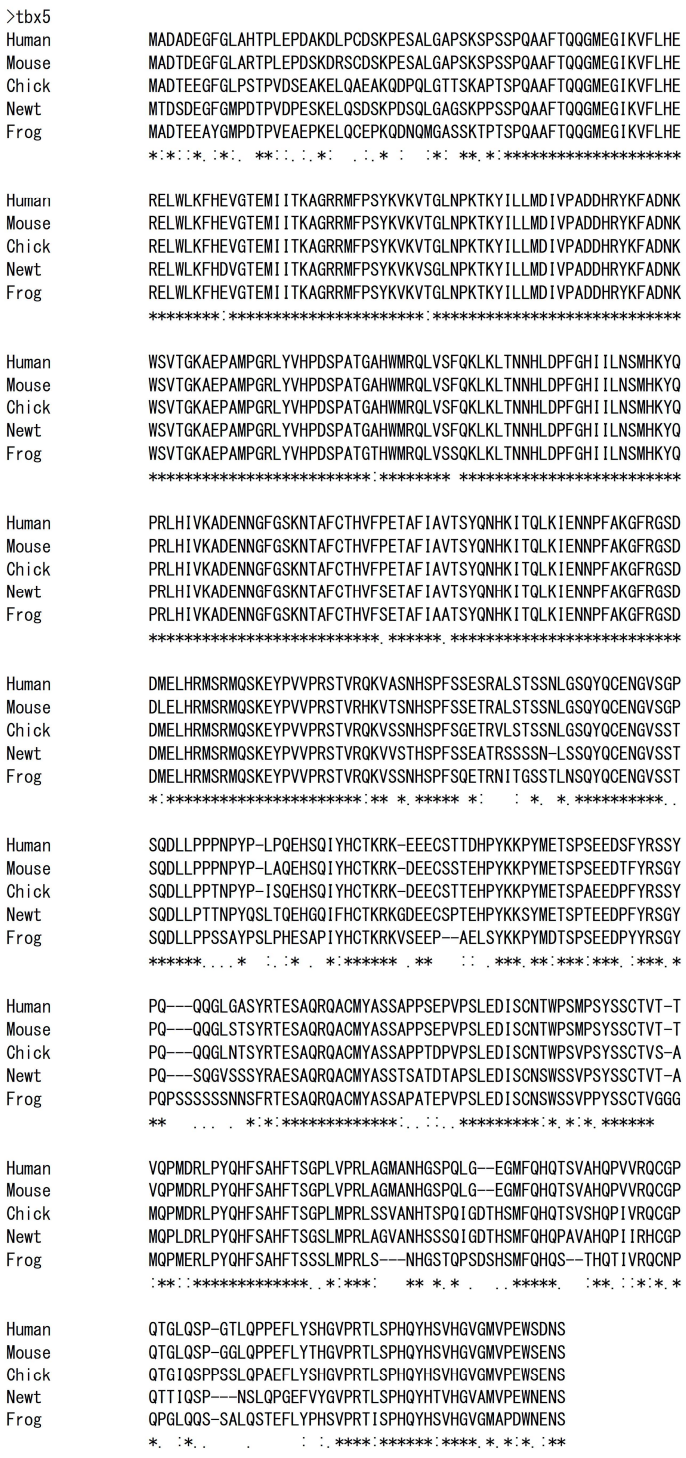

Figure I-3. comparisons of newt (*Pleurodeles waltl*), frog (*Xenopus tropicalis*), chick (*Gallus gallus*), mouse (*Mus musculus*) and human (*Homo sapiens*) amino acid sequences
Amino acid sequences are derived from UniprotKB or Xenbase. UniprotKB accession numbers and NCBI accession number (referenced in Xenbase) are listed at the top.

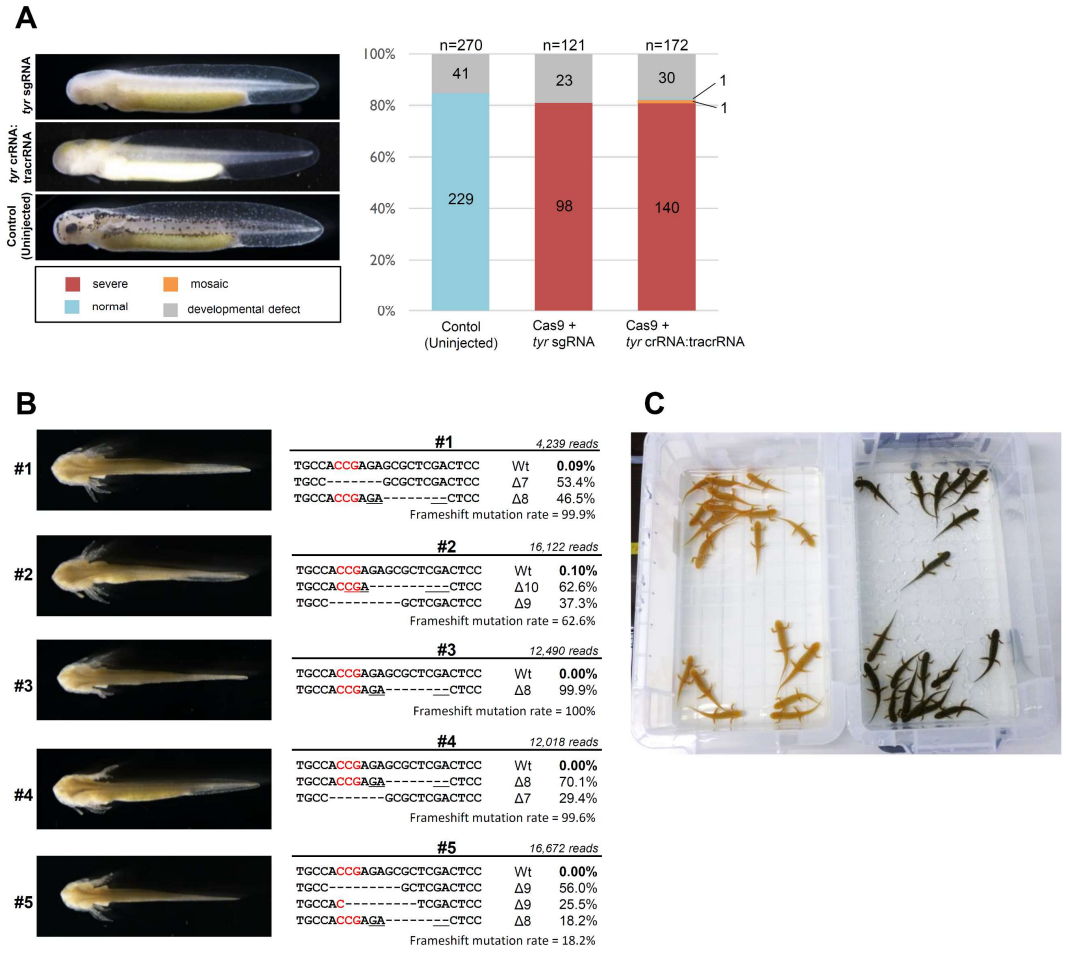

Figure I-4. Targeted gene disruption of *tyrosinase* (*tyr*) in *P. waltl*

(A) Representative phenotypes of *tyr* gRNAs/Cas9 protein-injected embryos (crispants) and their frequencies. Cas9 protein and sgRNA- (upper panel) or crRNA:tracrRNA-injected embryos (middle panel) showed almost complete albino phenotypes. The two gRNAs have the identical target sequence (Fig. I-2). Phenotypes are classified into three groups: severe, complete loss of pigmentation in retina pigmented epithelium (RPE); mosaic, partial loss of pigmentation in RPE; and normal, no alteration of pigmentation. Note that almost all surviving crispants showed a severe albino phenotype. Total and each group's sample sizes (n) are indicated at the top and middle of each graph, respectively. Each value was obtained from two independent experiments. (B) Genotypes of *tyr* crispants analyzed by amplicon sequencing. Representative mutant alleles, their occupancy rates, frameshift mutation rates, and total read counts are shown corresponding to each crispant (#1–5). Deletions are indicated by dashes. Protospacer adjacent motif (PAM) and microhomologous sequences are indicated by red letters and underscores, respectively. Less than 1% of wild-type alleles were found even though over ten thousand reads were sequenced, suggesting the saturation of mutagenesis in the founder. All mutant alleles and their frequencies are listed in Table I-1. (C) *tyr* crispant (left) and wild-type (uninjected controls; right) juveniles.

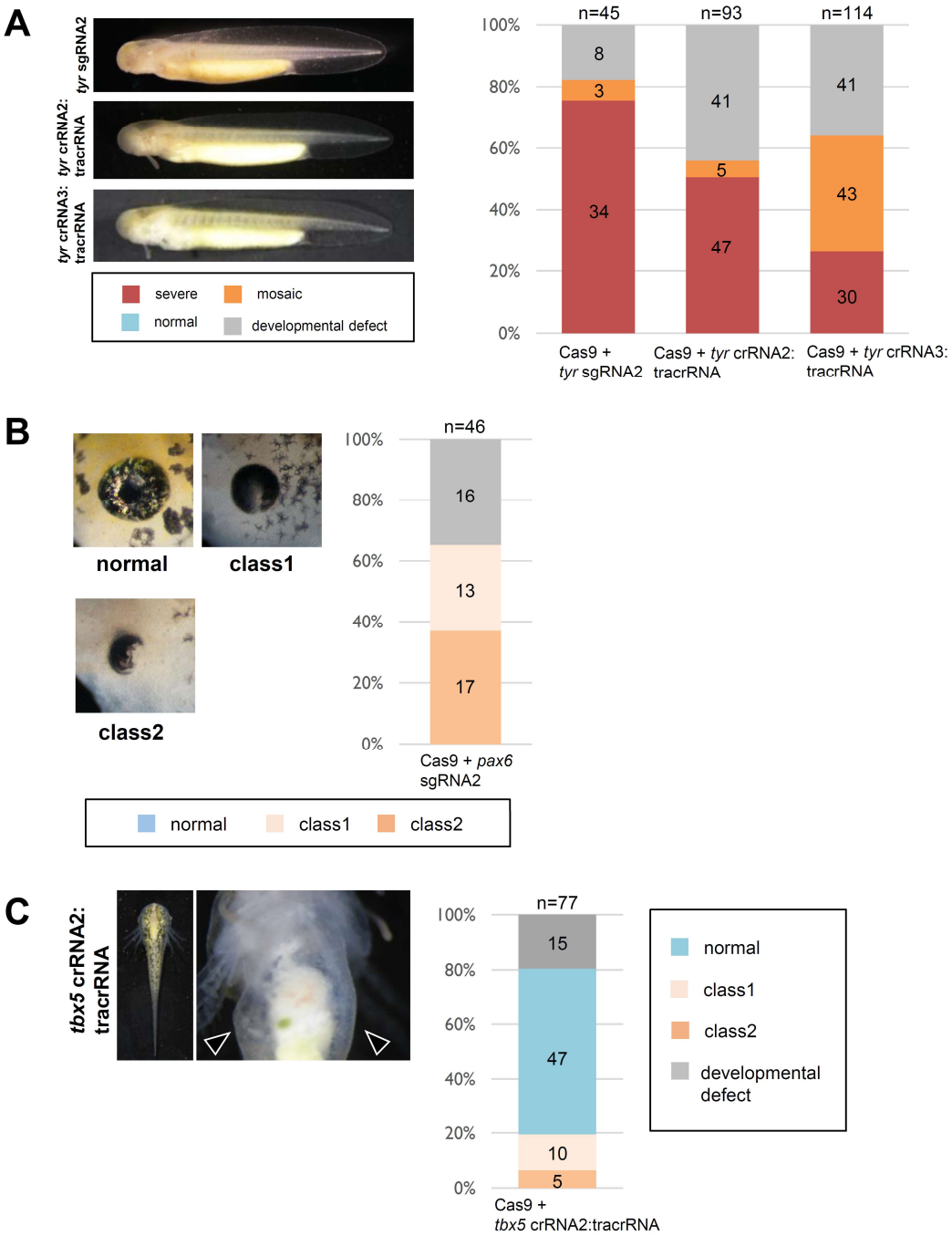

Figure I-5. phenocopy of *tyr*, *pax6* and *tbx5* using Cas9 RNP with other gRNAs
(A) Representative phenotypes of *tyr* crispants and the frequencies of phenotypes. In addition to *tyr* gRNA used in Fig. I-4A, I designed two gRNAs recognizing different sequences of *tyr*; *tyr* gRNA2 and 3. Both *tyr* gRNA2 and 3 led complete albino phenotype, same as *tyr* gRNA in Fig. I-4A. Target sequences of *tyr* sgRNA2 and *tyr* crRNA2 are identical. (B) Representative phenotypes of *pax6* crispants and the frequencies of phenotypes. Cas9 + *pax6* gRNA2 injected embryos showed eye malformation, same as *pax6* gRNA in Fig. I-7A. (C) Representative phenotypes of *tbx5* crispants and the frequencies of phenotypes. Cas9 + *tbx5* gRNA2 injected embryos had no detectable limb bud and showed abnormalities in their heart, same as Fig. I-8A. Arrow head indicates no limb bud formation in *tbx5* crispants. Total and each group sample size (n) are indicated at the top and the middle of each graph, respectively.

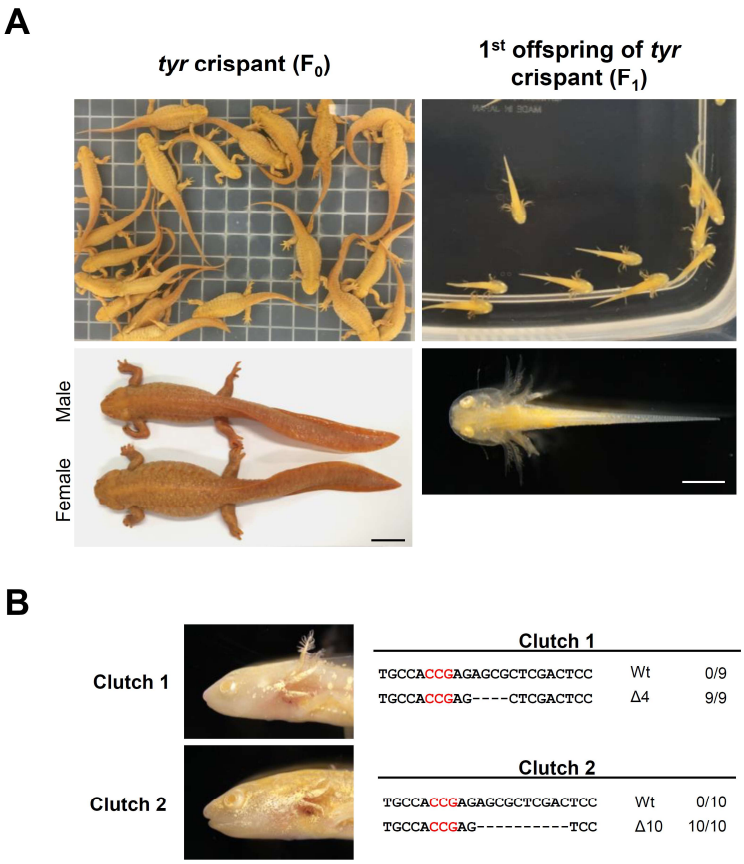

Figure I-6. Generation of F_1 offspring by crossing *tyr* crispants.
(A) Sexually mature *tyr* crispants (founders, F_0). From 50 juveniles (3 months postfertilization), 39 adults survived for 17 months and most of them reached sexual maturity within a year. Scale bar = 20 mm. The first F_1 offspring were obtained on 15 Aug, 2017, from the *tyr* crispants (F_0) established on 19 Aug, 2016. Scale bar = 2 mm. (B) Genotypes of *tyr* F_1 offspring from two clutches identified by Sanger sequencing. Deletions are indicated by dashes. The number of clones for each allele is indicated on the right. Sequences represent homozygous mutants in two albino clutches. PAM is indicated by red letters.

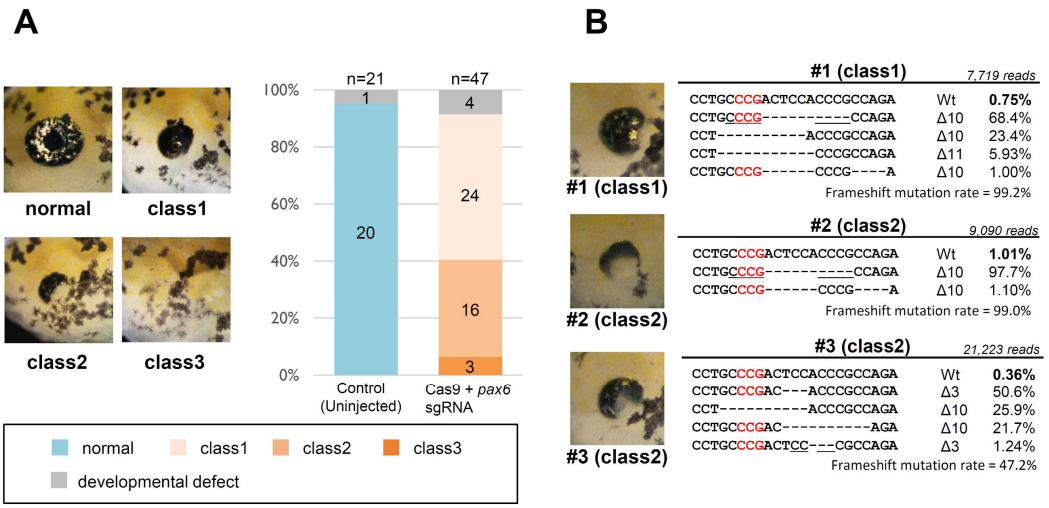

Figure I-7. Targeted gene disruption of *pax6*

(A) Representative phenotypes of *pax6* crispant and frequencies of phenotypes from two independent experiments. Phenotypes are classified into four groups, in accordance with a previous report (Yasue et al. 2017). All of the *pax6* crispants showed eye malformation. Total and each group's sample sizes (n) are indicated at the top and middle of each graph, respectively. (B) Genotypes of *pax6* crispants. Representative mutant alleles, their occupancy rates, frameshift mutation rates, and total read counts are shown corresponding to each embryo (#1–3). Deletions are indicated by dashes. PAM and microhomologous sequences are indicated by red letters and underscores, respectively. All mutant alleles and their frequencies are listed in Table I-1.

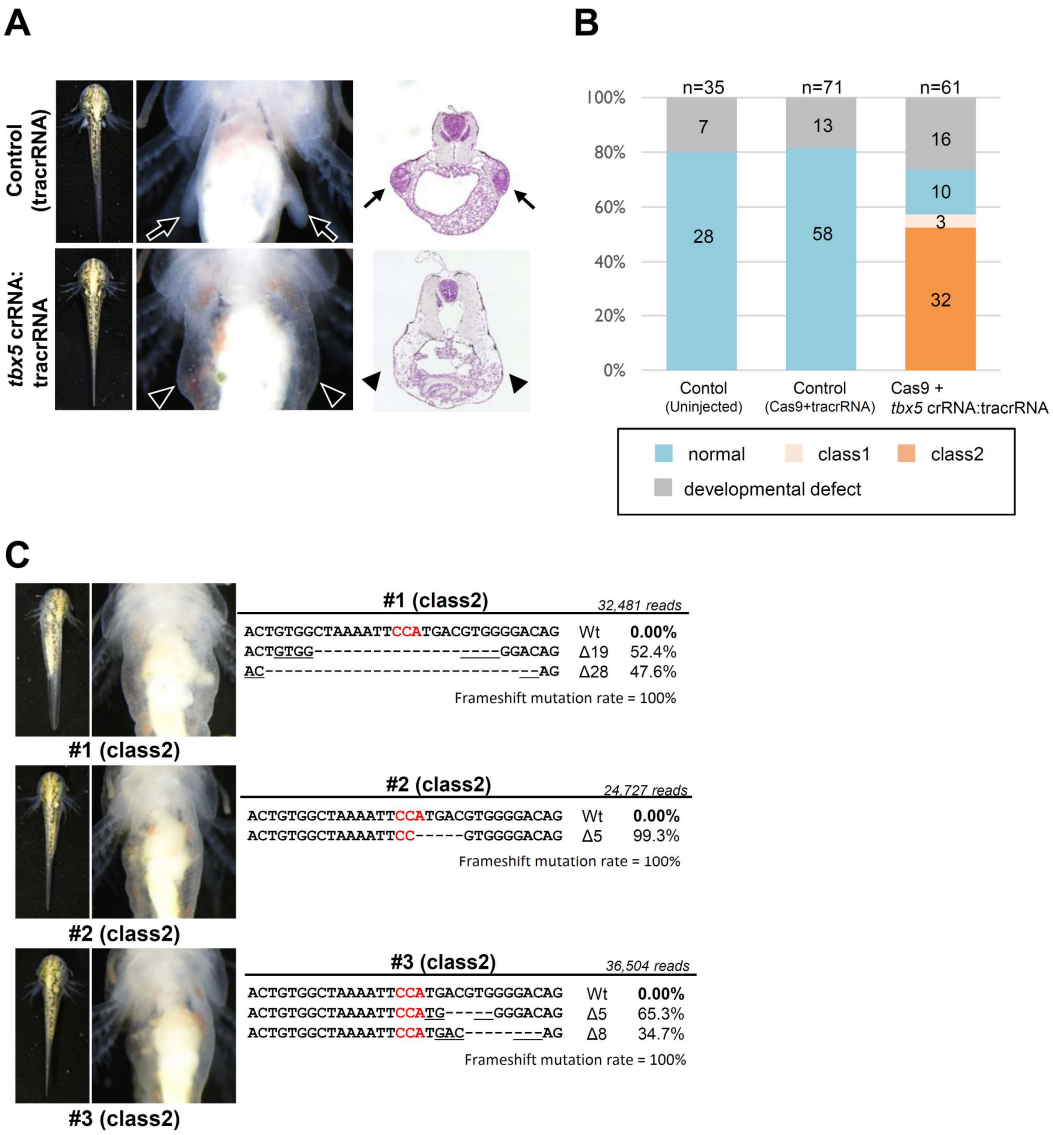

Figure I-8. Targeted gene disruption of *tbx5*

(A) A representative phenotype of *tbx5* crispant; dorsal view, ventral view, and cross section through the torso. Arrow and arrowhead indicate limb bud formation in the control and no limb bud formation in the *tbx5* crispant, respectively. (B) Frequencies of phenotypes from two independent experiments. Phenotypes are classified into two groups: class 1, limb defect only; and class 2, limb defect and heart abnormalities. Neither of the control experimental groups, uninjected and Cas9 protein with only tracrRNA injected (without *tbx5* crRNA), showed these phenotypes. (C) Genotypes of *tbx5* crispants. Representative mutant alleles, their occupancy rates, frameshift mutation rates, and total read counts are shown corresponding to each embryo (#1–3). Deletions are indicated by dashes. PAM and microhomologous sequences are indicated by red letters and underscores, respectively. All mutant alleles and their frequencies are listed in Table I-1.

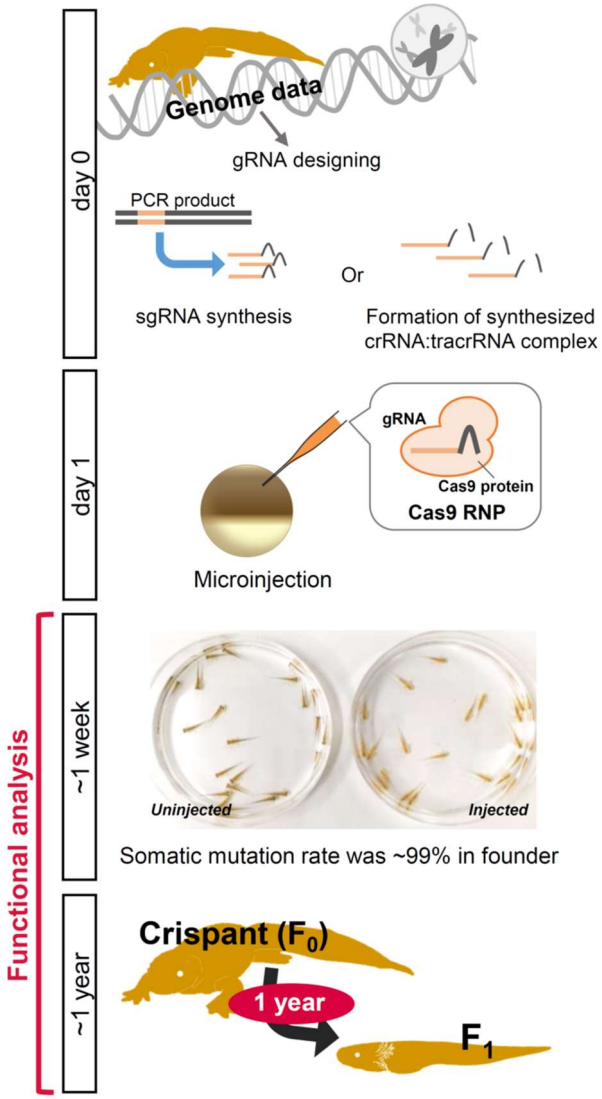

Figure I-9. A schematic diagram of crispants for functional analysis of coding and regulatory regions of *P. waltl* genes.

Table I-1. Amplicon sequencing data of on-targets

tyr_#1

CIGAR	Sequence	Inframe/Frameshift	Read count	Occupancy rate
70M7D77M	TTCAGCTCAGTGCC-------GCGCTCGACTCCTGGCCTATCTGAACCTGGCC	Frameshift	2263	53.4
77M8D69M	TTCAGCTCAGTGCCACCGAGA--------CTCCTGGCCTATCTGAACCTGGCC	Frameshift	1972	46.5
154M	TTCAGCTCAGTGCCACCGAGAGCGCTCGACTCCTGGCCTATCTGAACCTGGCC	Inframe	4	0.1
		Frameshift mutation rate =		99.9

tyr_#2

CIGAR	Sequence	Inframe/Frameshift	Read count	Occupancy rate
75M10D69M	TTCAGCTCAGTGCCACCGA----------CTCCTGGCCTATCTGAACCTGGCC	Frameshift	10090	62.6
70M9D75M	TTCAGCTCAGTGCC---------GCTCGACTCCTGGCCTATCTGAACCTGGCC	Inframe	6016	37.3
154M	TTCAGCTCAGTGCCACCGAGAGCGCTCGACTCCTGGCCTATCTGAACCTGGCC	Inframe	16	0.1
		Frameshift mutation rate =		62.6

tyr_#3

CIGAR	Sequence	Inframe/Frameshift	Read count	Occupancy rate
77M8D69M	TTCAGCTCAGTGCCACCGAGA--------CTCCTGGCCTATCTGAACCTGGCC	Frameshift	12474	99.9
75M10D69M	TTCAGCTCAGTGCCACCGA----------CTCCTGGCCTATCTGAACCTGGCC	Frameshift	16	0.1
		Frameshift mutation rate =		100.0

tyr_#4

CIGAR	Sequence	Inframe/Frameshift	Read count	Occupancy rate
77M8D69M	TTCAGCTCAGTGCCACCGAGA--------CTCCTGGCCTATCTGAACCTGGCC	Frameshift	8420	70.1
70M7D77M	TTCAGCTCAGTGCC-------GCGCTCGACTCCTGGCCTATCTGAACCTGGCC	Frameshift	3533	29.4
72M9D73M	TTCAGCTCAGTGCCAC---------TCGACTCCTGGCCTATCTGAACCTGGCC	Inframe	53	0.4
63M4I5M1I6M4I2M4I78	TTCAGCT++++CAGTG+CCACCG++++AG++++AGCGCTCGACTCCTGGCCTA	Frameshift	12	0.1
		Frameshift mutation rate =		99.6

tyr_#5

CIGAR	Sequence	Inframe/Frameshift	Read count	Occupancy rate
70M9D75M	TTCAGCTCAGTGCC---------GCTCGACTCCTGGCCTATCTGAACCTGGCC	Inframe	9341	56.0
72M9D73M	TTCAGCTCAGTGCCAC---------TCGACTCCTGGCCTATCTGAACCTGGCC	Inframe	4250	25.5
77M8D69M	TTCAGCTCAGTGCCACCGAGA--------CTCCTGGCCTATCTGAACCTGGCC	Frameshift	3041	18.2
66M7I4M13D71M	TTCAGCTCAG+++++++TGCC-------------GACTCCTGGCCTATCTGAA	Inframe	40	0.2
		Frameshift mutation rate =		18.2

pax6_#1

CIGAR	Sequence	Inframe/Frameshift	Read count	Occupancy rate
22M10D132M	ACGGCAGACCCCTGCCCG----------CCAGAAGATCGTGGAGCTCGCCCAC	Frameshift	5278	68.4
17M10D137M	ACGGCAGACCCCT----------ACCCGCCAGAAGATCGTGGAGCTCGCCCAC	Frameshift	1810	23.4
17M11D136M	ACGGCAGACCCCT-----------CCCGCCAGAAGATCGTGGAGCTCGCCCAC	Frameshift	458	5.9
22M6D4M4D128M	ACGGCAGACCCCTGCCCG------CCCG----AAGATCGTGGAGCTCGCCCAC	Frameshift	77	1.0
164M	ACGGCAGACCCCTGCCCGACTCCACCCGCCAGAAGATCGTGGAGCTCGCCCAC	Inframe	58	0.8
17M22I147M	ACGGCAGACCCCT++++++++++++++++++++++GCCCGACTCCACCCGCCA	Frameshift	15	0.2
65M10D89M	ACGGCAGACCCCTGCCCGACTCCACCCGCCAGAAGATCGTGGAGCTCGCCCAC	Frameshift	14	0.2
22M7D3M3D129M	ACGGCAGACCCCTGCCCG-------CCG---GAAGATCGTGGAGCTCGCCCAC	Frameshift	9	0.1
		Frameshift mutation rate =		99.2

pax6_#2

CIGAR	Sequence	Inframe/Frameshift	Read count	Occupancy rate
22M10D132M	ACGGCAGACCCCTGCCCG----------CCAGAAGATCGTGGAGCTCGCCCAC	Frameshift	8882	97.7
22M6D4M4D128M	ACGGCAGACCCCTGCCCG------CCCG----AAGATCGTGGAGCTCGCCCAC	Frameshift	100	1.1
164M	ACGGCAGACCCCTGCCCGACTCCACCCGCCAGAAGATCGTGGAGCTCGCCCAC	Inframe	92	1.0
17M9D3M11D4M2D3M7I2M4D4M9D8M1I5M3I8M9I12M10I2M36I9M19D5M10D18M	ACGGCAGACCCCT----------CAC-----------TCGT--AGC+++++++T	Frameshift	16	0.2
		Frameshift mutation rate =		99.0

pax6_#3

CIGAR	Sequence	Inframe/Frameshift	Read count	Occupancy rate
24M3D137M	ACGGCAGACCCCTGCCCGAC---ACCCGCCAGAAGATCGTGGAGCTCGCCCAC	Inframe	10738	50.6
17M10D137M	ACGGCAGACCCCT----------ACCCGCCAGAAGATCGTGGAGCTCGCCCAC	Frameshift	5495	25.9
24M10D130M	ACGGCAGACCCCTGCCCGAC----------AGAAGATCGTGGAGCTCGCCCAC	Frameshift	4600	21.7
27M3D134M	ACGGCAGACCCCTGCCCGACTCC---CGCCAGAAGATCGTGGAGCTCGCCCAC	Inframe	263	1.2
164M	ACGGCAGACCCCTGCCCGACTCCACCCGCCAGAAGATCGTGGAGCTCGCCCAC	Inframe	77	0.4
25M10D129M	ACGGCAGACCCCTGCCCGACT----------GAAGATCGTGGAGCTCGCCCAC	Frameshift	50	0.2
		Frameshift mutation rate =		47.8

tbx5_#1

n_deleted	Sequence	Inframe/Frameshift	Read count	Occupancy rate
19	ACTGTGG-------------------GGACAGAGATGATCATCACAAAGGCTG	Frameshift	17015	52.4
28	AC----------------------------AGAGATGATCATCACAAAGGCTG	Frameshift	15466	47.6
		Frameshift mutation rate =		100.0

tbx5_#2

n_deleted	Sequence	Inframe/Frameshift	Read count	Occupancy rate
5	ACTGTGGCTAAAATTCC-----GTGGGGACAGAGATGATCATCACAAAGGCTG	Frameshift	24547	99.3
5	ACTGTGGCTAAAATT-----ACGTGGGGACAGAGATGATCATCACAAAGGCTG	Frameshift	161	0.7
5	ACTGTGGCTAAAATTCCATG-----GGGACAGAGATGATCATCACAAAGGCTG	Frameshift	19	0.1
		Frameshift mutation rate =		100.0

tbx5_#3

n_deleted	Sequence	Inframe/Frameshift	Read count	Occupancy rate
5	ACTGTGGCTAAAATTCCATG-----GGGACAGAGATGATCATCACAAAGGCTG	Frameshift	23829	65.3
8	ACTGTGGCTAAAATTCCATGAC--------AGAGATGATCATCACAAAGGCTG	Frameshift	12675	34.7
		Frameshift mutation rate =		100.0

Table I-2. List of primers and crRNAs used in this study

gene	gRNA	usage	no.	F/R	sequence (5' to 3')
tyr	sgRNA (Fig. 1)	sgRNA template	-	F	TAATACGACTCACTATAGGCCAGGAGTCGAGCGCTCTGTTTTAGAGCTAGAAATAGCAAG
tyr	sgRNA2 (Fig. S4)	sgRNA template	-	F	TAATACGACTCACTATAGGCCGTTTGTGTGCTGCTGTGTTTTAGAGCTAGAAATAGCAAG
tyr	crRNA (Fig. 1)	crRNA	-	-	GGCCAGGAGUCGAGCGCUCUGUUUUAGAGCUAUGCU
tyr	crRNA2 (Fig. S4)	crRNA	-	-	GGCCGUUUGUGUGCUGCUGUGUUUUAGAGCUAUGCU
tyr	crRNA3 (Fig. S4)	crRNA	-	-	GGCUGAUGGUGCGCUUGGCCGUUUUAGAGCUAUGCU
pax6	sgRNA (Fig. 3)	sgRNA template	-	F	TAATACGACTCACTATAGGCGGGAGATGTCGCAGGGCGTTTTAGAGCTAGAAATAGCAAG
pax6	sgRNA2 (Fig. S4)	sgRNA template	-	F	TAATACGACTCACTATAGGTCTTCTGGCGGGTGGAGTGTTTTAGAGCTAGAAATAGCAAG
tbx5	crRNA (Fig. 4)	crRNA	-	-	UCAUCUCUGUCCCCACGUCAGUUUUAGAGCUAUGCU
tbx5	crRNA2 (Fig. S4)	crRNA	-	-	GGACGAGGGCUUUGGGAUGCGUUUUAGAGCUAUGCU
-	-	sgRNA template	-	R	AAAAGCACCGACTCGGTGCCACTTTTTCAAGTTGATAACGGACTAGCCTTATTTTAACTTGCTATTTC TAGCTCTAAAAC
tyr	-	amplicon-seq	1	F	TCGTCGGCAGCGTCAGATGTGTATAAGAGACAGATGCTGCGCCTTCGGGCGTTGGGGTCCGG
tyr	-	amplicon-seq	1	R	GTCTCGTGGGCTCGGAGATGTGTATAAGAGACAGGCATATCTGCTCGTAGGTCCCAGTGGCGA
tyr	-	amplicon-seq	2	F	TCGTCGGCAGCGTCAGATGTGTATAAGAGACAGTAGCTGCGCCTTCGGGCGTTGGGGTCCGG
tyr	-	amplicon-seq	2	R	GTCTCGTGGGCTCGGAGATGTGTATAAGAGACAGGCTAATCTGCTCGTAGGTCCCAGTGGCGA
tyr	-	amplicon-seq	3	F	TCGTCGGCAGCGTCAGATGTGTATAAGAGACAGCGATTGCGCCTTCGGGCGTTGGGGTCCGG
tyr	-	amplicon-seq	3	R	GTCTCGTGGGCTCGGAGATGTGTATAAGAGACAGATCGATCTGCTCGTAGGTCCCAGTGGCGA
tyr	-	amplicon-seq	4	F	TCGTCGGCAGCGTCAGATGTGTATAAGAGACAGGCTATGCGCCTTCGGGCGTTGGGGTCCGG
tyr	-	amplicon-seq	4	R	GTCTCGTGGGCTCGGAGATGTGTATAAGAGACAGTAGCATCTGCTCGTAGGTCCCAGTGGCGA
tyr	-	amplicon-seq	5	F	TCGTCGGCAGCGTCAGATGTGTATAAGAGACAGGGAGTGCGCCTTCGGGCGTTGGGGTCCGG
tyr	-	amplicon-seq	5	R	GTCTCGTGGGCTCGGAGATGTGTATAAGAGACAGCTCCATCTGCTCGTAGGTCCCAGTGGCGA
tyr	-	amplicon-seq	Wt-1	F	TCGTCGGCAGCGTCAGATGTGTATAAGAGACAGATGCTGCGCCTTCGGGCGTTGGGGTCCGG
tyr	-	amplicon-seq	Wt-1	R	GTCTCGTGGGCTCGGAGATGTGTATAAGAGACAGGCATATCTGCTCGTAGGTCCCAGTGGCGA
tyr	-	amplicon-seq	Wt-2	F	TCGTCGGCAGCGTCAGATGTGTATAAGAGACAGTAGCTGCGCCTTCGGGCGTTGGGGTCCGG
tyr	-	amplicon-seq	Wt-2	R	GTCTCGTGGGCTCGGAGATGTGTATAAGAGACAGGCTAATCTGCTCGTAGGTCCCAGTGGCGA
tyr	-	amplicon-seq	Wt-3	F	TCGTCGGCAGCGTCAGATGTGTATAAGAGACAGCGATTGCGCCTTCGGGCGTTGGGGTCCGG
tyr	-	amplicon-seq	Wt-3	R	GTCTCGTGGGCTCGGAGATGTGTATAAGAGACAGATCGATCTGCTCGTAGGTCCCAGTGGCGA
tyr	-	amplicon-seq	Wt-4	F	TCGTCGGCAGCGTCAGATGTGTATAAGAGACAGGCTATGCGCCTTCGGGCGTTGGGGTCCGG
tyr	-	amplicon-seq	Wt-4	R	GTCTCGTGGGCTCGGAGATGTGTATAAGAGACAGTAGCATCTGCTCGTAGGTCCCAGTGGCGA
pax6	-	amplicon-seq	1	F	TCGTCGGCAGCGTCAGATGTGTATAAGAGACAGATGCGAGTGTTCGTGAACGGCAGACCCCT
pax6	-	amplicon-seq	1	R	GTCTCGTGGGCTCGGAGATGTGTATAAGAGACAGGCATGCGCGAGTTCGTGTGCTAAAGTGCA
pax6	-	amplicon-seq	2	F	TCGTCGGCAGCGTCAGATGTGTATAAGAGACAGTAGCGAGTGTTCGTGAACGGCAGACCCCT
pax6	-	amplicon-seq	2	R	GTCTCGTGGGCTCGGAGATGTGTATAAGAGACAGGCTAGCGCGAGTTCGTGTGCTAAAGTGCA
pax6	-	amplicon-seq	3	F	TCGTCGGCAGCGTCAGATGTGTATAAGAGACAGGCATGAGTGTTCGTGAACGGCAGACCCCT
pax6	-	amplicon-seq	3	R	GTCTCGTGGGCTCGGAGATGTGTATAAGAGACAGATGCGCGCGAGTTCGTGTGCTAAAGTGCA
pax6	-	amplicon-seq	Wt	F	TCGTCGGCAGCGTCAGATGTGTATAAGAGACAGCGTTGAGTGTTCGTGAACGGCAGACCCCT
pax6	-	amplicon-seq	Wt	R	GTCTCGTGGGCTCGGAGATGTGTATAAGAGACAGAACGGCGCGAGTTCGTGTGCTAAAGTGCA
tbx5	-	amplicon-seq	-	F	TCGTCGGCAGCGTCAGATGTGTATAAGAGACAGGTGGAATGGCCTAGCCGTAATAAAGC
tbx5	-	amplicon-seq	-	R	GTCTCGTGGGCTCGGAGATGTGTATAAGAGACAGAAACATGTATGTACAAATATTGTTTACCTTCCAG
tyr (F1)	-	cloning	-	F	TCGTCGGCAGCGTCAGATGTGTATAAGAGACAGATGCTGCGCCTTCGGGCGTTGGGGTCCGG
tyr (F1)	-	cloning	-	R	GTCTCGTGGGCTCGGAGATGTGTATAAGAGACAGGCATATCTGCTCGTAGGTCCCAGTGGCGA
tyr (F1)	-	sequencing	-	F	GTAAAACGACGGCCAGT

CHAPTER Ⅱ

Functional analysis of a limb-specific enhancer of *shh* gene in newt regeneration

Introduction

Shh is a morphogen responsible for the polarizing activity of limb bud. Part of the posterior region in forming limb bud is defined as the ZPA, which expresses *Shh*, an organizer of the anterior–posterior patterning of developing limbs. ZPA transplantation and *Shh* misexpression at the anterior region limb bud resulted in duplicated and polydactyly limb in a cell-mass- or dose-dependent manner (Tickle 1981; Yang et al. 1997). Moreover, distal to the stylopod, AP patterning is severely disrupted in *Shh* knockout mouse, demonstrating that Shh is the determinant of posteriorization in developing limb (Chiang et al. 1996; Chiang et al. 2001).

The precise spatiotemporal expression of *Shh* in the limb bud is regulated by the ZRS (also known as MFCS1; Lettice et al. 2003, Sagai et al. 2005). Deletion of the ZRS causes complete loss of limb-specific *Shh* expression and mutant embryos show distally truncated limbs that are equivalent to the phenotypes of *Shh* KO embryos (Sagai et al. 2005). In addition, more than 20 different sites of point mutations in the ZRS associated with limb malformations, such as pre-axial polydactyly, have been reported in multiple species including humans (Hill et al. 2003; Hill and Lettice 2013).

From a comparative and functional genomic analysis among vertebrates including snakes, a 17-bp snake-specific deletion in ZRS was identified (Kvon et al. 2016). This 17-bp sequence is specifically deleted in multiple species of snake but present in limbed tetrapods and fish, and is indispensable for proper *Shh* expression and digit formation (Kvon et al. 2016). The 17-bp sequence contains an ETS1 transcription factor binding site. ETS1 binds multiple ETS recognition sites in the ZRS and has been suggested to activate *Shh* expression directly; however, loss of the ETS1 site in the 17-bp

sequence alone did not impair *Shh* expression in limb bud (Lettice et al. 2012).

In Chapter II, I targeted a potentially critical site in the limb-specific enhancer of *shh*, and evaluated its function in the development and regeneration of *P. waltl*. Perturbation of ZRS decreased mRNA expression and led to severe defects in digit patterning during regeneration. In addition, this incomplete regeneration was caused by small deletions at the 17-bp snake-specific deletion site without perturbation of the ETS1 binding site, suggesting that another transcription factor binding motif is involved in limb development and regeneration.

Materials and Methods

Animals

The Iberian ribbed newts used in this study were maintained in a closed colony following their original purchase from Tao (Chiba, Japan) in 2010. The animals were reared as described previously (Hayashi et al. 2013), unless stated otherwise. For anesthesia before limb regeneration, MS-222 (Sigma) was used at a final concentration of 0.02%. Animal rearing and treatments were performed and approved in accordance with Guidelines for the Use and Care of Experimental Animals and the Institutional Animal Care and Use Committee of Hiroshima University.

Sequencing of target genes and ZRS locus

The ZRS locus of *P. waltl* was sequenced after inverse PCR cloning of this locus using the primers listed in Table II-2. The partial genomic sequences and amplicon sequencing data of ZRS have been deposited in GenBank (LC378706) and the DDBJ Sequence Read Archive (DRA006550). The cDNA sequence for RT-qPCR was predicted from the *P. waltl* transcriptome data set (Elewa et al. 2017) and resequenced (Fig. II-5).

VISTA global alignments

Comparison of *P. waltl* ZRS genomic sequences with other species was performed using the mVISTA program (Frazer et al. 2004; http://genome.lbl.gov/vista/) based on LAGAN multiple alignments (Brudno et al. 2003), using the default parameters. The genomic DNA sequences analyzed here are shown in Fig. II-1.

Preparation of gRNAs

gRNAs were designed using CRISPR-direct (Naito et al. 2015). For sgRNA preparation, templates were assembled by a PCR-based strategy (Sakane et al. 2017). The oligonucleotide information is listed in Table II-2. DNA templates were purified with a QIAquick PCR Purification Kit (Qiagen); subsequently, sgRNAs were synthesized *in vitro* using a MEGA Shortscript T7 Kit and purified using a MEGA Clear Kit (Thermo Fisher Scientific).

Microinjection

Microinjection was performed based on previously reported protocols (Hayashi et al. 2014; Hayashi and Takeuchi, 2016; Sakane et al. 2017; Sakane et al. 2018). A brief description of this protocol with minor modification is presented below. The fertilized eggs were treated with 0.5% cysteine in 0.1×MMR for 30 s to remove the jelly. De-jellied eggs were rinsed in 0.1× MMR and transferred into injection medium [5% Ficoll in 0.3× MMR]. The eggshells were removed using forceps and stored at 8°C in injection medium until microinjection. Two nanogram of recombinant Cas9 protein (Alt-R *S.p.* Cas9 Nuclease 3NLS; IDT) and 200 pg of each sgRNA (400 pg in total) in 150 mM KCl and 20 mM HEPES buffer were co-injected into one-cell-stage embryos using Nanoject II (Drummond). After microinjection, the embryos were incubated overnight at 25°C in injection medium and then transferred into 0.1× MMR.

Genotyping

Genomic DNA was extracted from amputated limb of ZRS crispants (n=11) using DNeasy Blood and Tissue Kit (Qiagen), individually. Uninjected samples were also collected. An amplicon-sequencing library was prepared based on the Illumina "16S Metagenomic Sequencing Library Preparation." For the first round of PCR, the target regions containing gRNA targeting sites were amplified from individual genomic DNA of uninjected embryos and ZRS crispants, using KOD FX Neo (TOYOBO) with primer sets containing barcode and overhang adaptor sequences. Each PCR product was purified using a QIAquick PCR Purification Kit (Qiagen) and equal quantities of PCR products were pooled and re-purified using the same kit. Then, each PCR product underwent the second round of PCR using different index primer sets. The second round of PCR was performed to construct a sequence library using a Nextra XT index kit (Illumina). The final library was purified and sequenced on Illumina MiSeq. Library construction and sequencing were performed at Microgen Japan. Amplicon-sequencing data were analyzed in accordance with the work of Sakane et al. (2018). PCR and Illumina sequence error rates were determined using uninjected samples, and then mutant reads were counted using an in-house script in R (version 3.3.3; Table II-1). All primers are listed in Table II-2.

Limb regeneration

Crispant or uninjected larvae were separated into single cases before the feeding stage and reared individually for one month. Larvae were anesthetized with 0.02% MS-222.

Then, the left forelimbs were amputated with a surgical knife at the middle of the forearm level. Each amputated limb was stored at −20°C until genomic DNA extraction for amplicon sequencing. The number of digits was counted when uninjected control larvae completed regeneration, at 18 days postamputation (dpa). A small spike structure was not counted as representing a regenerating digit.

RNA extraction and RT-qPCR

Forelimbs of crispant and uninjected larvae were amputated as described above, and then medium-bud-stage blastema (Iten and Bryant, 1973) was collected at 7 dpa. Tissues were incubated overnight in RNAlater (Thermo Fisher Scientific) at 4°C, and stored at −80°C after removing the solution. Total RNA was isolated from each sample by using NucleoSpin RNA Plus XS with rDNase Set (TaKaRa Bio, Shiga, Japan). The same amount of total RNA (20 ng) was reverse-transcribed and pre-amplified using CellAmp Whole Transcriptome Amplification Kit (TaKaRa Bio). qPCR was carried out by using SYBR Premix Ex Taq II (TaKaRa Bio) with a Step One real-time PCR system (Thermo Fisher Scientific). The copy numbers of each gene were quantified using pCRII-TOPO-Pw*shh* vector and purified PCR product of Pw*gapdh* as standards, and subsequently relative *shh* expression levels were normalized by *gapdh*. Two technical replicates were used per sample. All primers are listed in Table II-2. Primer sets for qPCR were designed by Primer 3 (Untergasser et al. 2012). The statistical significance of differences was calculated by the Mann–Whitney U-test using EZR software (Kanda, 2013).

Results

Cloning and sequencing of P. waltl ZRS locus and comparison to other vertebrates

To identify the ZRS in newt, a genomic fragment from *P. waltl* containing the ZRS locus was sequenced after inverse PCR cloning using the primers listed in Table II-2 (Fig. II-1). I next compared this sequence with the core ~800 bp of mouse ZRS enhancer [chr5: 29,314,881–29,315,667 (mm10)] and the orthologous sequences from human [chr7: 156,791,087–156,791,875 (hg38)], python [13056–13925 (*Python_molurus_bivittatus*-5.0.2-2355.6)] and cobra [589764–590624 (*Ophiophagus hannah* scaffold183.1)], whose activities were confirmed by a transgenic mouse enhancer reporter assay (Kvon et al. 2016). Global pairwise alignment was carried out using LAGAN (Brudno et al. 2003), and the results were visualized using the VISTA Browser (Frazer et al. 2004; Fig. II-2). I found high overall conservation of noncoding DNA among human, mouse, python, and *P. waltl*. In contrast, a 17-bp snake-specific deletion site, which is specifically deleted in multiple species of snake and present in limbed tetrapods and fish (Kvon et al. 2016), showed lower conservation to python and cobra, as expected (Fig. II-2).

ZRS function in limb development

To evaluate ZRS function in limb development, I targeted the 17-bp snake-specific deletion, a potentially critical site in the ZRS since it was shown to be able to resurrect the snake ZRS enhancer function in mouse (Kvon et al. 2016). I designed two sgRNAs adjacent to the 17-bp snake-specific deletion site of ZRS in the *P. waltl* genome to excise

out this sequence (Fig. II-1-2), and co-injected them into one-cell-stage embryos. Regarding limb development, both forelimb and hindlimb of ZRS crispants seemed to develop normally, without limb truncation like in ZRS-deleted mouse (Sagai et al. 2005) and mouse with its original ZRS replaced by snake ZRS (Kvon et al. 2016). Most of the ZRS crispants formed four digits in forelimb, the same as in the wild-type, whereas 7 of 33 larvae formed only three digits (Fig. II-3A; left column).

ZRS function in limb regeneration

To investigate further, I amputated the forelimb of ZRS crispants and evaluated ZRS function in regeneration. Unlike in development, digit formation was severely disrupted in regeneration; specifically, approximately half of ZRS crispants failed to complete regeneration, while wild-type larvae regenerated their digits completely (Fig. II-3A; right column). Notably, the formation of one or two digits was seen only in ZRS crispants. I observed a one-digit-regenerated ZRS crispant for 13 months, but it failed to regenerate the other digits at the end of this period (Fig. II-4), suggesting that this phenotype reflects impaired regeneration but not delayed regeneration. Genomic DNA was extracted from the amputated limb and genotyped individually for each phenotype (Fig. II-3B, Table II-1). Entire deletion of the 17-bp sequence did not occur as I expected, even in cases of defective regeneration; however, all analyzed alleles had an insertion or deletion (indel) at the ZRS sgRNA2 cleavage site (Fig. II-3B, Table II-1).

Quantification of shh expression level during limb regeneration

To examine whether ZRS perturbation affected the *shh* expression in regeneration, I quantified the *shh* expression level by RT-qPCR. Forelimbs of ZRS crispant (n=21) and uninjected siblings (n=16) were amputated, and then medium-bud-stage blastema was collected at 7 dpa (Iten and Bryant, 1973), individually. To prepare the standards for quantification of the copy numbers of each gene, *shh* and *gapdh* cDNA sequences were predicted from the *P. waltl* transcriptome data set (Elewa et al., 2017) and resequenced (Fig. II-5). *shh* relative mRNA level was measured by RT-qPCR and normalized to the level of *gapdh*. As expected, using Mann–Whitney U-test, *shh* expression of ZRS crispants appeared to be significantly lower in blastema than in the wild-type (Fig. II-6).

Discussion

Functional assessment of noncoding regulatory elements is important to understand how genes are up- or downregulated in a precise spatiotemporal manner during development and regeneration. The CRISPR-Cas9 system also allows us to investigate their function easily *in vivo*, not only the functions of protein-coding genes (Han et al. 2015; Burger et al. 2016). I designed a pair of gRNAs adjacent to the 17-bp snake-specific deletion site to excise out this sequence; however, they did not remove it. Optimization of the distance of two gRNAs would be needed when using offset gRNAs (Ran et al. 2013), but I was unable to design another gRNA due to the very small region of interest. Even though the deletion of ZRS was only 4–5 bp, it caused severe digit deformation in regeneration. Meanwhile, a large 120-bp deletion was occasionally seen (~10%). Such large deletions occur in association with programmable nucleases (Shin et al. 2017): when double-strand breaks at the target site are mainly repaired by the non-homologous end joining (NHEJ) pathway, endogenous nucleases could occasionally create large deletions.

I demonstrated that CRISPR-mediated perturbation of ZRS decreased *shh* mRNA expression and led to defects in digit patterning during regeneration. Similar phenotypes of digit loss were also seen in regenerating limb treated with cyclopamine, a *shh* signaling inhibitor, in a dose-dependent manner (Roy and Gardiner 2002), supporting the view that the failure of limb regeneration in the ZRS crispant was caused by insufficient reactivation of *shh*. Notably, ZRS-perturbed newts showed variability in their regenerating ability; some of them regenerated their limbs normally, despite possessing similar mutations at the on-target site. Variation of limb phenotype upon ZRS perturbation was also reported to be seen in ZRS 3′-end-deleted mouse (Lettice et al. 2014) and mouse

carrying human ZRS (in which the endogenous mouse ZRS had been replaced with human ZRS; Kvon et al. 2016). Even point mutations in ZRS would be a factor that weakens or strengthens *cis–trans* interaction, consequently subtly altering *shh* expression (Williamson et al. 2011; Lettice et al. 2017). This subtle alteration can lead to stochastic variability of phenotypes associated with ZRS mutations (Hill, 2007; Symmons et al. 2016). Therefore, the variability in limb phenotype in ZRS crispants may reflect subtle alteration of the *shh* expression rather than allele complexity or mosaicism in the founder. I speculate that low levels of *shh* signaling in ZPA stochastically affected digit number in regeneration. In addition, ZRS perturbation may also subtly alter spatio-temporal expression of *shh* and affect digit patterning (Shapiro et al. 2003). Intriguingly, even a few base deletions at the 17-bp snake-specific deletion site resulted in impaired limb regeneration, revealing that the small site (ZRS sgRNA2 targeting sequence) plays a crucial role in the reactivation of *shh*. This site contains predicted homeodomain DNA motifs, implying that the mutation disrupted Hox binding (Leal and Cohn 2016).

>P.waltl_ZRS

ccgtgcattaaatatcccacgtgcgacagcacatcctgactaattacccaaattacccagacatccttccaaaaagccgcgaagcaacagagagc

gagtctgtcggattaaaaggttaactcctaaaacatcaaacgagcgccagataataaaagccaatcgcacagaaatttgaggtaacttccttgct

taattaatgaggtgggccaggtggagcgaagaggcccgcgctggtgcgcaggccgccaataaagctgaacaacatgacaacacaatagaggagaa

acaacgatttttaatatgcgtctatcctgtgtcacagtttgaaattgtcctggtttatgtccctttggcaaagttacataaaagtgaccctgt

actgtattttatggccagatgacttttcttttgttcccggtgactaatttggatcaggccccgccatcttaaatagacacagaaatgaggtcgg

gagagtgaggctgtctgtctcagtatggtttcattgcatttttttcattattttggctttttttttgctacagatcatccataaatggctggaaat

gagtgattaaggaagtgctgcttagtgttagtggcacatgaacattctttgttagtttttcccccttttgtgggtgagaggaaatcctgtactg

cagaaacaataaggaaacctcctgctgggaacctttcaaagagctgtaacctgcgcacttttttttaatctcggtttccatacacaatacgctgt

gatatttcaacagctattttcacgtcagacaccctacatgggctgacgtgaaaatagctgtt

Figure II-1. Genomic sequence of *P. waltl* ZRS
gRNA target protospacer and PAM sequence are marked in gray and red, respectively.

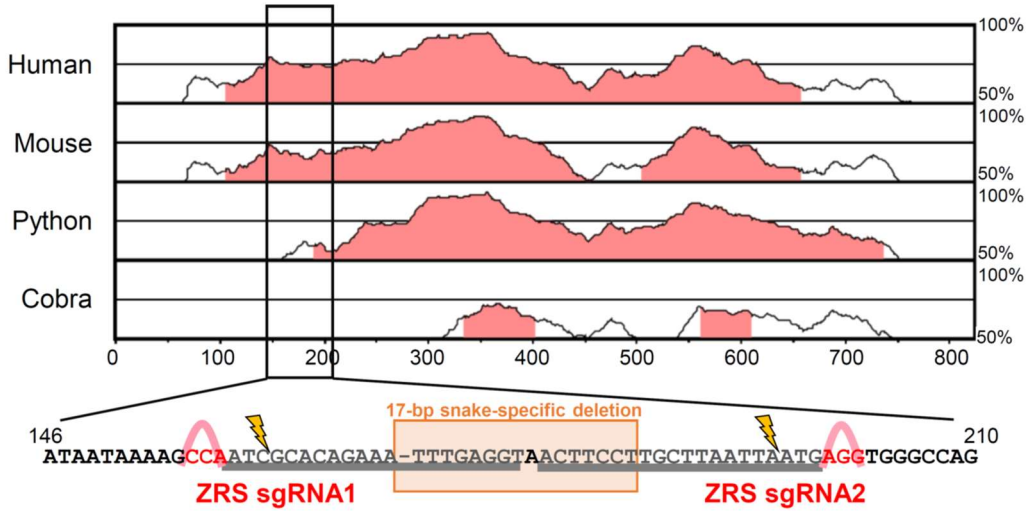

Figure II-2. The VISTA plot of the zone of polarizing activity regulatory sequence (ZRS)
The plot shows conserved sequences between *P. waltl* and human, mouse, and snakes (python and cobra). Horizontal axis: *P. waltl* sequence, vertical axis: percentage identity in a 100-bp window. The conserved non-coding sequences with >70% identity over 100 bp are highlighted in pink under the curve. Putative 17-bp snake-specific deletions in *P. waltl* ZRS and sgRNA target sequences are shown below the plot. sgRNA target and PAM sequence are marked in gray and red, respectively.

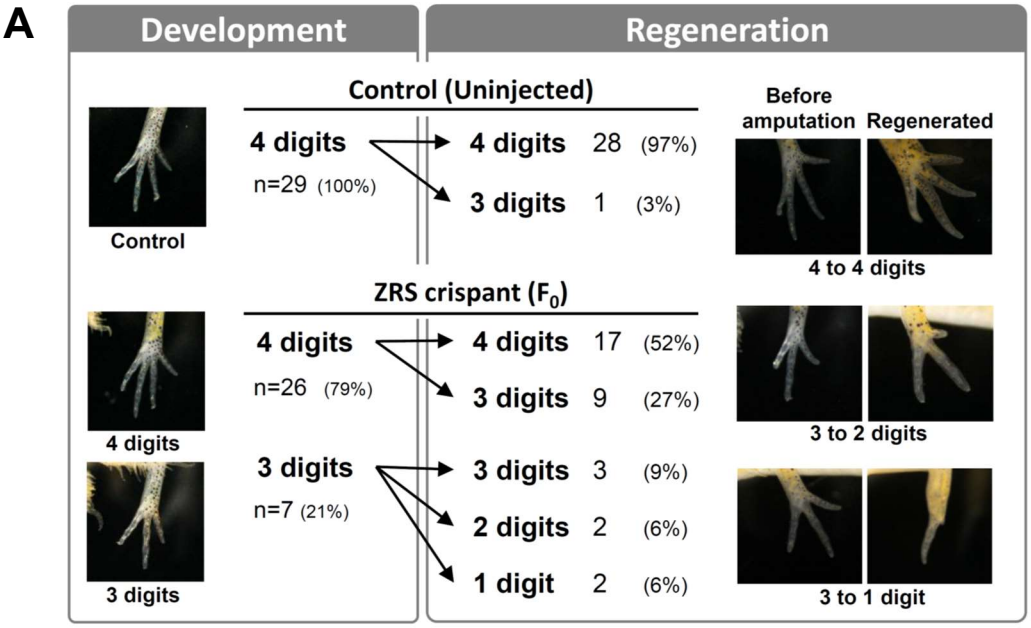

B

#1 (3 to 1 digit) *11,063 reads*

TTCCTTGCTTAATTAATGAGGTG	Wt	0.00%
TTCCTTGCTTAAT----GAGGTG	Δ4	67.0%
TTCCTTGCTTAATT---GAGGTG	Δ3	33.0%

#2 (3 to 1 digit) *10,361 reads*

TTCCTTGCTTAATTAATGAGGTG	Wt	0.00%
TTCCTTGCTTAAT----GAGGTG	Δ4	61.5%
TTCCTTGCTTAATT---GAGGTG	Δ3	25.0%
----------	Δ120	13.5%

#3 (3 to 2 digits) *9,394 reads*

TTCCTTGCTTAATTAATGAGGTG	Wt	0.00%
TTCCTTGCTTAATT--------G	Δ8	47.8%
TTCCTTGCTTAAT---------G	Δ9	42.9%
TTCCTTGCTTAAT----GAGGTG	Δ4	9.31%

#4 (3 to 2 digits) *31,113 reads*

TTCCTTGCTTAATTAATGAGGTG	Wt	0.00%
----------	Δ120	100%

Figure II-3. Targeted cis-regulatory element disruption of the limb enhancer of *sonic hedgehog*
(A) Left column: Phenotypes of ZRS crispants in limb development (1-month postfertilization). Most of the ZRS crispants developed limbs normally and 7 of 33 larvae showed the loss of one digit. Numbers of digits of left forelimbs and their frequencies are shown. Right column: Phenotypes of ZRS crispants in limb regeneration. Unlike in limb development, severe reduction of digit formation was seen. In addition, approximately half of ZRS-disrupted larvae could not regenerate their digits completely. Numbers of regenerated digits and their frequencies are shown. (B) Genotypes of ZRS crispants with severe phenotypes. Genomic DNA was extracted from each amputated limb (#1-4) and the target genomic locus was sequenced. Representative mutant alleles, their occupancy rates, and total read counts are shown. Deletions are indicated by dashes. PAM, part of the 17-bp snake-specific deletion site, and microhomologous sequences are indicated by red and yellow letters, and underscores, respectively. Genotypes of other larvae with moderate phenotypes, all mutant alleles, and their frequencies are listed in Table II-1.

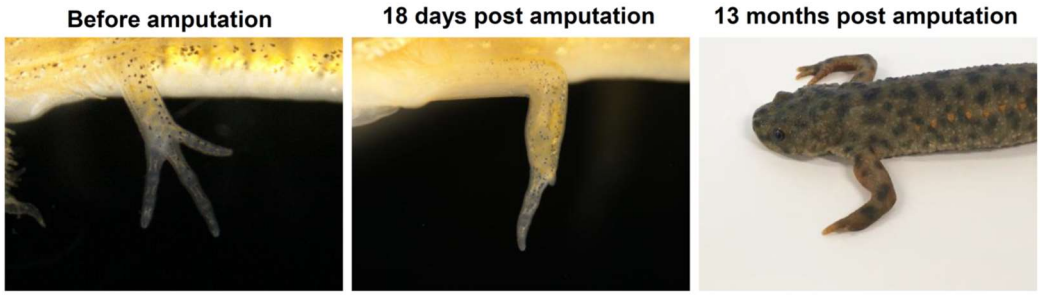

Figure II-4. Longer observation of ZRS crispant regeneration

>Pw*shh*

GCTTTTTGTCCCCTGTTGCTGTCTTGACACCGAACTCCGATGTGTTTGGC
TGTCAGCGCCCAGAGAGCTTGTCTTTTCAGCACCTGCTCGGATAGGGACC
GGCGAATGGTGCGGCACTGAAACGGGCAGCAGATACGGGACCAGTTGGTG
CGCGCGAGGGGCCAGCAGCACAAGTACCGCGGACCGAGGGTGGGGGGAGT
TCGCGAGCCCTGTATGGACGAGATGATGCTGCTGAGGCGAGTCCTGCTGG
GGGGCTTCATCTGCGCCCTCCTAGTGCCCTCGGGGCTGGGCTGCGGTCCG
GGCAGAGGCATTGGCCAGAGGAGACGCCCCAAGAAGCTTACTCCGTTGGC
ATACAAGCAGTTCATCCCCAACGTGGCCGAGAAGACCCTGGGGGCCAGTG
GACGTTATGAGGGCAAGATCACGCGCAACTCGGAGCGCTTCAAGGAGCTA
ACTCCTAATTACAACCCTGACATTATATTTAAGGACGAGGAGAACACGGG
AGCGGATAGGCTGATGACCCAGAGGTGTAAGGATAAGCTGAATGCCCTGG
CAATCTCGGTGATGAACCAGTGGCCTGGAGTCAAGCTGAGGGTCACCGAA
GGTTGGGACGAGGACGGCCACCACTCTGAGGAGTCCCTGCACTATGAGGG
TCGGGCAGTGGACATCACCACCTCAGACCGGGACCGCAGCAAGTATGGCA
TGCTGGCCCGCCTGGCTGTGGAGGCTGGCTTCGACTGGGTCTACTTTGAG
TCCAAGGCCCACATCCACTGCTCAGTGAAAGCAGAGAACTCAGTAGCTGT
AAAATCGGGAGGTTGCTTCCCAGGTTCTGCCACGGTGACCCTGGAGCAAG
GGGTGAGGATTCCCGTGAAGGACTTGAAGCCGGGGAACAGGGTGCTCGCC
GTGGACGTTGAGGGCAGGCTGATTTACAGCGACTTTCTCTTGTTCATGGA
CAAGGAAGAGACGGTCAGAAAAGTCTTCTACGTGATAGAGACCTCCCTGC
CTCGGGAGAGGCTCCGCCTGACCGCCGCCCACCTCCTCTTTGTAGCCCAA
GAGCACCCAGGAAACGCCAGTGCGGGCAACTTCCGGTCCAAGTTTGGCAG
CGCCGGTTTCCGGTCCATGTTCGCCAGCAGCGTGCGGCCTGGACACCGGG
TGCTCACGGAGGACCGGGAAGGCCGGGGGCTAAGGGAAGCCACGGTGGAT
CGAGTGTACCTGGAGGAGGCCACAGGGGCCTACGCTCCCGTCACTGCGCA
CGGGACCGTGGTCATAGACAGGGTGCTGGCCTCTTGTTACGCGGTCATAG
AGGAACACAGCTGGGCGCACTGGGCCTTCGCCCCTCTGAGAGTGGGCTTC
GGTATTTTGTCATTCTTCTCTCCCCAAGACTATTCCAGCCATTCCCCGCC
AGCGCCCTCTCAGGCAGAGGGAGTCCACTGGTACTCAGAGATCCTCTACC
GGATAGGGACATGGGTGTTACAGGCGGACACGATCCACCCATTGGGAATG
GCAGCGAAGTCCAGCTGAAAACCAGTCTGGGAGCCAGTATAAAGACTTAA
GAGAAATTTAAACAAAAGTAGGACTGTCCAAAGTAGACTTTAAGTAAACA
AAGACCCAGAAAGTTTGTTTTTCTTTGTTGTGTTTTATACTTTTATTGAT
GTAGTCTTTACCTGTTCCGTTGTTCCCTTGGCTGTTGGATAT

>Pw*gapdh*

GGCAAACTTGTAATCAACGGCCAGCCCATCACAATCTTCCAAGAACGTGA
CCCCACCAACATCAAGTGGGGGGATGCTGGAGCAGACTACGTGGTTGAGT
CGACTGGAGTGTTCACCACCATTGACAAAGCATCTGCTCATCTGAAGGGT
GGCGCCAAACGTGTGATCATCTCCGCCCCTTCTGCTGACGCTCCCATGTT
TGTGATGGGAGTAAACCACGAGAAGTACGACAAGTCCCTGAAGGTAGTAA
GCAACGCCTCCTGCACTACAAACTGTCTGGCTCCTCTGGCTAAGGTCATC
CACGACAACTTTCACATCGTCGAGGGTTTGATGACCACTGTACATGCTGT
GACAGCTACACAAAAGACTGTGGACGGTCCTTCTGGGAAACTGTGGCGTG
ACGGCAGAGGTGCCAATCAGAATATCATTCCAGCCTCTACCGGGGCAGCC
AAGGCCGTGGGCAAAGTTATTCCTGAACTCAATGGGAAACTCACAGGCAT
GGCCTTCCGTGTACCTGTCCCCAATGTGTCTGTGGTTGACCTGACCTGCC
GCTTGGAGAAGGCTGCCTCATATGACGACATTAAGAAGGTGGTAAAGGCA
GCAGCTGATGGACCAATGAAAGGAATTTTGGGATACACCGAGGAACAGGT
GGTGTCCTCCGACTTCAACGGTGACGATCACTCATCAATCTTTGATGCTG
GTGCCGGTATTGCACTCAACGACCACTTTGTGAAACTGGTTTCTTGGTAT
GACAATGAATTTGGTTACAGTCAACGCGTTGTGGATCTGATGAGTCACAT
GGCCAGCAAGGAATAG

Figure II-5. partial cDNA sequences of the genes for qPCR
Underline indicates primer sequence for qPCR.

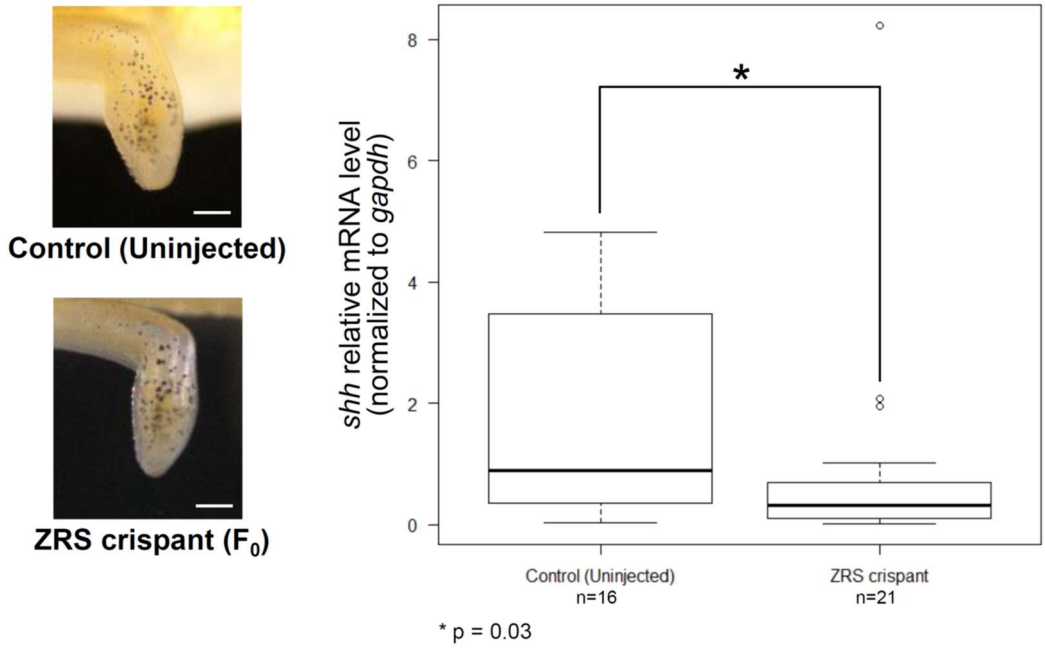

Figure II-6. Quantitative analysis of *shh* expression in regenerating ZRS crispants.
Left panel: The left forelimbs were amputated at the middle of the forearm level and regenerating blastemas were collected at 7 days postamputation. Scale bar = 500 µm. Right panel: Boxplot of *shh* mRNA level in each blastema from wild-type (n=16) and ZRS crispant (n=21) relative to *gapdh* measured by RT-qPCR. *shh* expression was significantly decreased in ZRS crispant (*: Mann–Whitney U-test, p=0.03).

Table II-1. Amplicon sequencing data of on-targets

ZRS_#1_3to1digit

CIGAR	Sequence	Read count	Occupancy rate
225M4D190M	CCAATCGCACAGAAATTTGAGGTAACTTCCTTGCTTAAT----GAGGTGGGCCAGGT	7408	67.0
226M3D190M	CCAATCGCACAGAAATTTGAGGTAACTTCCTTGCTTAATT---GAGGTGGGCCAGGT	3655	33.0

ZRS_#2_3to1digit

CIGAR	Sequence	Read count	Occupancy rate
225M4D190M	CCAATCGCACAGAAATTTGAGGTAACTTCCTTGCTTAAT----GAGGTGGGCCAGGT	6375	61.5
226M3D190M	CCAATCGCACAGAAATTTGAGGTAACTTCCTTGCTTAATT---GAGGTGGGCCAGGT	2584	24.9
140M120D159M	----------	1402	13.5

ZRS_#3_3to2digits

CIGAR	Sequence	Read count	Occupancy rate
226M8D185M	CCAATCGCACAGAAATTTGAGGTAACTTCCTTGCTTAATT--------GGGCCAGGT	4489	47.8
225M9D185M	CCAATCGCACAGAAATTTGAGGTAACTTCCTTGCTTAAT---------GGGCCAGGT	4030	42.9
225M4D190M	CCAATCGCACAGAAATTTGAGGTAACTTCCTTGCTTAAT----GAGGTGGGCCAGGT	875	9.3

ZRS_#4_3to2digits

CIGAR	Sequence	Read count	Occupancy rate
140M120D159M	----------	31133	100.0

ZRS_#5_3to3digits

CIGAR	Sequence	Read count	Occupancy rate
225M4D190M	CCAATCGCACAGAAATTTGAGGTAACTTCCTTGCTTAAT----GAGGTGGGCCAGGT	6617	76.2
226M3D190M	CCAATCGCACAGAAATTTGAGGTAACTTCCTTGCTTAATT---GAGGTGGGCCAGGT	2067	23.8

ZRS_#6_3to3digits

CIGAR	Sequence	Read count	Occupancy rate
225M4D190M	CCAATCGCACAGAAATTTGAGGTAACTTCCTTGCTTAAT----GAGGTGGGCCAGGT	8375	76.3
226M3D190M	CCAATCGCACAGAAATTTGAGGTAACTTCCTTGCTTAATT---GAGGTGGGCCAGGT	2607	23.7

ZRS_#7_4to3digits

CIGAR	Sequence	Read count	Occupancy rate
219M16D184M	CCAATCGCACAGAAATTTGAGGTAACTTCCTTG----------------GGCCAGGT	12623	100.0

ZRS_#8_4to3digits

CIGAR	Sequence	Read count	Occupancy rate
226M3D190M	CCAATCGCACAGAAATTTGAGGTAACTTCCTTGCTTAATT---GAGGTGGGCCAGGT	4979	89.1
225M4D190M	CCAATCGCACAGAAATTTGAGGTAACTTCCTTGCTTAAT----GAGGTGGGCCAGGT	609	10.9

ZRS_#9_4to4digits

CIGAR	Sequence	Read count	Occupancy rate
225M4D190M	CCAATCGCACAGAAATTTGAGGTAACTTCCTTGCTTAAT----GAGGTGGGCCAGGT	10592	82.0
226M3D190M	CCAATCGCACAGAAATTTGAGGTAACTTCCTTGCTTAATT---GAGGTGGGCCAGGT	2324	18.0

ZRS_#10_4to4digits

CIGAR	Sequence	Read count	Occupancy rate
228M1I191M	CCAATCGCACAGAAATTTGAGGTAACTTCCTTGCTTAATTAA+TGAGGTGGGCCAGG	3061	44.8
225M4D190M	CCAATCGCACAGAAATTTGAGGTAACTTCCTTGCTTAAT----GAGGTGGGCCAGGT	2566	37.5
224M3D192M	CCAATCGCACAGAAATTTGAGGTAACTTCCTTGCTTAA---ATGAGGTGGGCCAGGT	1208	17.7

ZRS_#11_4to4digits

CIGAR	Sequence	Read count	Occupancy rate
225M4D190M	CCAATCGCACAGAAATTTGAGGTAACTTCCTTGCTTAAT----GAGGTGGGCCAGGT	6831	71.0
226M3D190M	CCAATCGCACAGAAATTTGAGGTAACTTCCTTGCTTAATT---GAGGTGGGCCAGGT	2787	29.0

Table II-2. List of primers used in this study

gene	gRNA	usage	no.	F/R	sequence (5' to 3')
ZRS	sgRNA1 (Fig. 5)	sgRNA template	-	F	TAATACGACTCACTATAGGCTCAAATTTCTGTGCGATGTTTTAGAGCTAGAAATAGCAAG
ZRS	sgRNA2 (Fig. 5)	sgRNA template	-	F	TAATACGACTCACTATAGGTTCCTTGCTTAATTAATGGTTTTAGAGCTAGAAATAGCAAG
-	-	sgRNA template	-	R	AAAAGCACCGACTCGGTGCCACTTTTTCAAGTTGATAACGGACTAGCCTTATTTTAACTTGCTA TTTCTAGCTCTAAAAC
ZRS	-	amplicon-seq	1	F	TCGTCGGCAGCGTCAGATGTGTATAAGAGACAGATGCTGGGTTCTACCTTCATATGTCGATC
ZRS	-	amplicon-seq	2	F	TCGTCGGCAGCGTCAGATGTGTATAAGAGACAGTAGCTGGGTTCTACCTTCATATGTCGATC
ZRS	-	amplicon-seq	3	F	TCGTCGGCAGCGTCAGATGTGTATAAGAGACAGGCATTGGGTTCTACCTTCATATGTCGATC
ZRS	-	amplicon-seq	4	F	TCGTCGGCAGCGTCAGATGTGTATAAGAGACAGTTCGTGGGTTCTACCTTCATATGTCGATC
ZRS	-	amplicon-seq	5	F	TCGTCGGCAGCGTCAGATGTGTATAAGAGACAGGGCCTGGGTTCTACCTTCATATGTCGATC
ZRS	-	amplicon-seq	6	F	TCGTCGGCAGCGTCAGATGTGTATAAGAGACAGCCGGTGGGTTCTACCTTCATATGTCGATC
ZRS	-	amplicon-seq	7	F	TCGTCGGCAGCGTCAGATGTGTATAAGAGACAGAGTATGGGTTCTACCTTCATATGTCGATC
ZRS	-	amplicon-seq	8	F	TCGTCGGCAGCGTCAGATGTGTATAAGAGACAGCATATGGGTTCTACCTTCATATGTCGATC
ZRS	-	amplicon-seq	9	F	TCGTCGGCAGCGTCAGATGTGTATAAGAGACAGGATTTGGGTTCTACCTTCATATGTCGATC
ZRS	-	amplicon-seq	10	F	TCGTCGGCAGCGTCAGATGTGTATAAGAGACAGACTTTGGGTTCTACCTTCATATGTCGATC
ZRS	-	amplicon-seq	11	F	TCGTCGGCAGCGTCAGATGTGTATAAGAGACAGGAGATGGGTTCTACCTTCATATGTCGATC
ZRS	-	amplicon-seq	Wt	F	TCGTCGGCAGCGTCAGATGTGTATAAGAGACAGAATCTGGGTTCTACCTTCATATGTCGATC
ZRS	-	amplicon-seq	-	R	GTCTCGTGGGCTCGGAGATGTGTATAAGAGACAGGCATGGCCATAAAATACAGTACAGGGTCA
ZRS	-	inverse PCR	-	F	TTTTTTTAATCTCGGTTTCCATACACAATACGCTG
ZRS	-	inverse PCR	-	R	ACCTCAAATTTCTGTGCGATTGGCTTTTATTATCT
ZRS	-	sequencing	-	-	ATTGTAATACGACTCACTATAGGG
ZRS	-	sequencing	-	-	CAGGAAACAGCTATGACCATGATT
shh	-	cloning	-	F	GCTTTTTGTCCCCTGTTGCTGTCTT
shh	-	cloning	-	R	ATATCCAACAGCCAAGGGAACAACG
gapdh	-	qPCR standard	-	F	GGCAAACTTGTAATCAACGGCCAGC
gapdh	-	qPCR standard	-	R	CTATTCCTTGCTGGCCATGTGACTC
shh	-	qPCR	-	F	TGGTACTCAGAGATCCTCTACCG
shh	-	qPCR	-	R	TATACTGGCTCCCAGACTGGTT
gapdh	-	qPCR	-	F	TGACGATCACTCATCAATCTTTG
gapdh	-	qPCR	-	R	GTTGACTGTAACCAAATTCATTGTC

GENERAL CONCLUSIONS

Urodele amphibians have remarkable regenerative ability, which can morphologically and functionally restore their lost organs. The mechanism behind this regenerative ability has been studied for centuries using limb regeneration as a model. However, the mechanism of limb regeneration remains unclear. In this thesis, to decipher the involved mechanism, I focused on *shh* regulation, which plays an essential role in organ regeneration. Although epigenetic regulation of *shh* via ZRS is related to the loss of regenerative ability in anuran amphibians (Yakushiji et al. 2007), the involvement of ZRS in limb regeneration has not yet been functionally analyzed. In this study, I targeted and disrupted the 17-bp snake-specific deletion site in ZRS and found that mutations of this site severely affected limb regeneration. This is the first study involving functional analysis of the transcriptional regulatory sequence evoked by CRISPR-Cas9 in amphibian regeneration.

In Chapter I, I presented an efficient method of gene knockout using Cas9 RNP in *P. waltl*, which is suitable for regenerative biology studies with reverse genetics approaches. Most of the founders exhibited severe phenotypes associated with each target gene (*tyr*, *pax6*, *tbx5*); notably, all *tyr* Cas9 RNP-injected embryos showed complete albinism. Moreover, amplicon sequencing analysis of Cas9 RNP-injected embryos revealed virtually complete biallelic disruption at target loci in founders called “crispants,” allowing direct and rapid phenotypic analysis in the F_0 generation. In addition, I demonstrated the generation of *tyr* null F_1 offspring within a year. Recently, rapid advances of next-generation sequencing technology and assembly algorithms have enabled reading of the gigantic genome of salamanders (Elewa et al. 2017; Nowoshilow

et al. 2018). Therefore, this crispant assay can be applied to analyze hundreds of regeneration-related genes and contribute to understanding the regenerative ability of salamanders in the post-genomic era.

In Chapter II, using an efficient gene knockout strategy, I demonstrated that CRISPR-Cas-mediated perturbation of ZRS decreased *shh* mRNA expression and led to defects in digit patterning during not only development but also regeneration. I found that a deletion of even a few bases at the 17-bp snake-specific deletion site resulted in impaired limb regeneration. Similar phenotypes of digit loss were also reported in regenerating salamander limb treated with cyclopamine, an *shh* signaling inhibitor (Roy and Gardiner 2002; Singh et al. 2012), suggesting the possibility that the failure of limb regeneration was caused by insufficient reactivation of *shh* through ZRS perturbation.

The results presented in this thesis reveal that the small site in ZRS plays a crucial role in the reactivation of *shh* during limb regeneration. This site contains predicted Hox binding motifs, which have been implicated in ZRS regulation (Kmita et al. 2005; Capellini et al. 2006). Indeed, the substitution rate of homeodomain DNA motifs in the snake ZRS that lost its limb enhancer activity was shown to be higher than those of tetrapods (Kvon et al. 2016). In particular, luciferase reporter analysis of mouse ZRS series demonstrated that HOXD protein strongly transactivates ZRS, and snake-specific mutations disrupt its activation (Leal and Cohn 2016). Therefore, I speculate that the small mutation in ZRS disrupted Hox binding and decreased *shh* expression (Fig. 1).

In conclusion, I demonstrated that ZRS induces *shh* expression in regeneration, and the small site in ZRS plays a crucial role in ZRS activation. I hypothesize that *shh* is regulated by ZRS through trans-activator binding to the homeodomain DNA motif, and its sufficient expression ensures the functioning of the molecular circuitry in blastema for

correct regeneration.

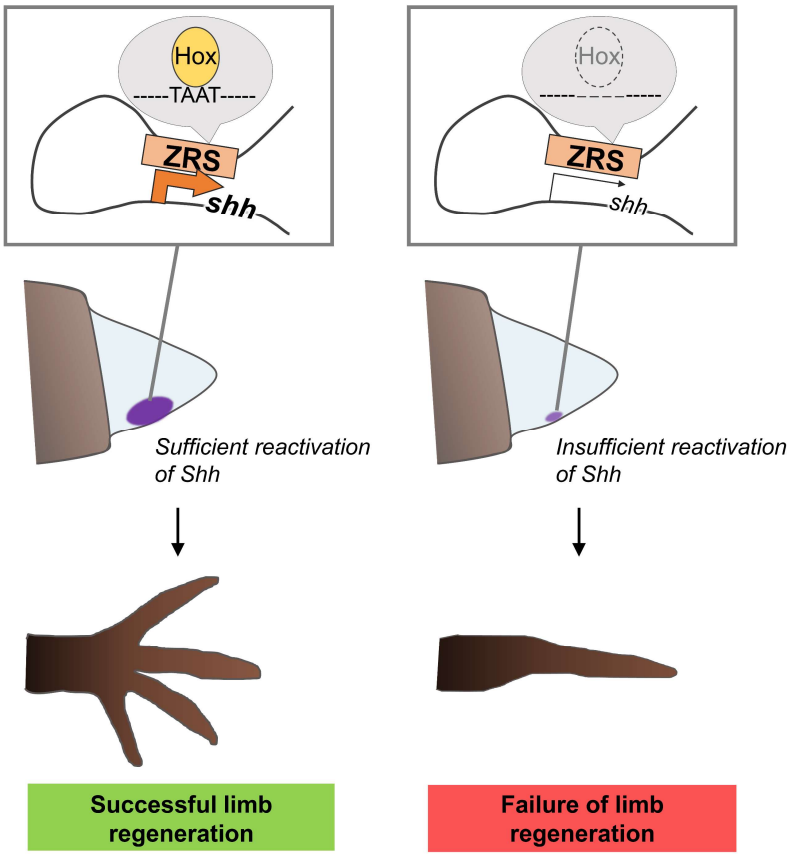

Figure 1. Schematic of the role of regulatory element in limb regeneration

Acknowledgments

This study was carried out at the Molecular Genetics Laboratory, Department of Mathematical and Life Sciences, Graduate School of Science, Hiroshima University. I would like to express my sincere gratitude to my supervisor, Professor Takashi Yamamoto, for providing me the chance to perform this study as a Ph.D. student in his laboratory. I would also like to express my deep appreciation to Dr. Ken-ichi T. Suzuki for his patient guidance, considerable encouragement, and invaluable discussions that contributed extensively to this research. I am very grateful to Dr. Toshinori Hayashi, Tottori University, for providing newts, giving advice on animal manipulation, and for his collaboration. I would also like to thank Dr. Takeshi Inoue and Professor Kiyokazu Agata, Gakushuin University, Ms. Miki Hirayama, Kyoto University, and Ms. Mie Nakajima, Tottori University, for their help. I wish to thank Ms. Miyuzu Suzuki and Dr. Shuji Shigenobu, National Institute for Basic Biology, for their kind help with the amplicon sequencing. I would also like to thank Dr. Midori Iida for advice on the bioinformatic analysis. This work was supported by the Japan Society for the Promotion of Science (JSPS) KAKENHI grant number 17J04796 (Grant-in-Aid for JSPS Fellows).

References

Ablain, J., Durand, E. M., Yang, S., Zhou, Y. and Zon, L. I. (2015). A CRISPR/Cas9 vector system for tissue-specific gene disruption in zebrafish. *Dev Cell* **32**, 756-764.

Agarwal, P., Wylie, J. N., Galceran, J., Arkhitko, O., Li, C., Deng, C., Grosschedl, R. and Bruneau, B. G. (2003). *Tbx5* is essential for forelimb bud initiation following patterning of the limb field in the mouse embryo. *Development* **130**, 623-633.

Ansai, S. and Kinoshita, M. (2014). Targeted mutagenesis using CRISPR/Cas system in medaka. *Biol Open* **3**, 362-371.

Barbosa-Sabanero, K., Hoffmann, A., Judge, C., Lightcap, N., Tsonis, P. A. and Del Rio-Tsonis, K. (2012). Lens and retina regeneration: new perspectives from model organisms. *Biochem J* **447**, 321-334.

Bassett, A. R., Tibbit, C., Ponting, C. P. and Liu, J. L. (2013). Highly efficient targeted mutagenesis of *Drosophila* with the CRISPR/Cas9 system. *Cell Rep* **4**, 220-228.

Brockes, J. P. and Kumar, A. (2002). Plasticity and reprogramming of differentiated cells in amphibian regeneration. *Nat Rev Mol Cell Biol* **3**, 566-574.

Brudno, M., Do, C. B., Cooper, G. M., Kim, M. F., Davydov, E., Green, E. D., Sidow, A., Batzoglou, S. and Program, N. C. S. (2003). LAGAN and Multi-LAGAN: efficient

tools for large-scale multiple alignment of genomic DNA. *Genome Res* **13**, 721-731.

Bruneau, B. G., Nemer, G., Schmitt, J. P., Charron, F., Robitaille, L., Caron, S., Conner, D. A., Gessler, M., Nemer, M., Seidman, C. E., et al. (2001). A murine model of Holt-Oram syndrome defines roles of the T-box transcription factor Tbx5 in cardiogenesis and disease. *Cell* **106**, 709-721.

Bryant, D. M., Johnson, K., DiTommaso, T., Tickle, T., Couger, M. B., Payzin-Dogru, D., Lee, T. J., Leigh, N. D., Kuo, T. H., Davis, F. G., et al. (2017). A tissue-mapped axolotl *de novo* transcriptome enables identification of limb regeneration factors. *Cell Rep* **18**, 762-776.

Bryant, S. V., Endo, T. and Gardiner, D. M. (2002). Vertebrate limb regeneration and the origin of limb stem cells. *Int J Dev Biol* **46**, 887-896.

Burger, A., Lindsay, H., Felker, A., Hess, C., Anders, C., Chiavacci, E., Zaugg, J., Weber, L. M., Catena, R., Jinek, M., et al. (2016). Maximizing mutagenesis with solubilized CRISPR-Cas9 ribonucleoprotein complexes. *Development* **143**, 2025-2037.

Burkard, C., Lillico, S. G., Reid, E., Jackson, B., Mileham, A. J., Ait-Ali, T., Whitelaw, C. B. and Archibald, A. L. (2017). Precision engineering for PRRSV resistance in pigs: Macrophages from genome edited pigs lacking CD163 SRCR5 domain are fully resistant to both PRRSV genotypes while maintaining biological function. *PLoS Pathog* **13**, e1006206.

Capellini, T. D., Di Giacomo, G., Salsi, V., Brendolan, A., Ferretti, E., Srivastava, D., Zappavigna, V. and Selleri, L. (2006). *Pbx1/Pbx2* requirement for distal limb patterning is mediated by the hierarchical control of Hox gene spatial distribution and *Shh* expression. *Development* **133**, 2263-2273.

Chang, N., Sun, C., Gao, L., Zhu, D., Xu, X., Zhu, X., Xiong, J. W. and Xi, J. J. (2013). Genome editing with RNA-guided Cas9 nuclease in zebrafish embryos. *Cell Res* **23**, 465-472.

Chiang, C., Litingtung, Y., Harris, M. P., Simandl, B. K., Li, Y., Beachy, P. A. and Fallon, J. F. (2001). Manifestation of the limb prepattern: limb development in the absence of sonic hedgehog function. *Dev Biol* **236**, 421-435.

Chiang, C., Litingtung, Y., Lee, E., Young, K. E., Corden, J. L., Westphal, H. and Beachy, P. A. (1996). Cyclopia and defective axial patterning in mice lacking Sonic hedgehog gene function. *Nature* **383**, 407-413.

Edvardsen, R. B., Leininger, S., Kleppe, L., Skaftnesmo, K. O. and Wargelius, A. (2014). Targeted mutagenesis in Atlantic salmon (Salmo salar L.) using the CRISPR/Cas9 system induces complete knockout individuals in the F_0 generation. *PLoS One* **9**, e108622.

Elewa, A., Wang, H., Talavera-López, C., Joven, A., Brito, G., Kumar, A., Hameed, L. S., Penrad-Mobayed, M., Yao, Z., Zamani, N., et al. (2017). Reading and editing the

Pleurodeles waltl genome reveals novel features of tetrapod regeneration. *Nat Commun* **8**, 2286.

Endo, T., Tamura, K. and Ide, H. (2000). Analysis of gene expressions during *Xenopus* forelimb regeneration. *Dev Biol* **220**, 296-306.

Endo, T., Yokoyama, H., Tamura, K. and Ide, H. (1997). *Shh* expression in developing and regenerating limb buds of *Xenopus laevis*. *Dev Dyn* **209**, 227-232.

Fei, J. F., Schuez, M., Tazaki, A., Taniguchi, Y., Roensch, K. and Tanaka, E. M. (2014). CRISPR-mediated genomic deletion of Sox2 in the axolotl shows a requirement in spinal cord neural stem cell amplification during tail regeneration. *Stem Cell Reports* **3**, 444-459.

Flowers, G. P., Timberlake, A. T., McLean, K. C., Monaghan, J. R. and Crews, C. M. (2014). Highly efficient targeted mutagenesis in axolotl using Cas9 RNA-guided nuclease. *Development* **141**, 2165-2171.

Frazer, K. A., Pachter, L., Poliakov, A., Rubin, E. M. and Dubchak, I. (2004). VISTA: computational tools for comparative genomics. *Nucleic Acids Res* **32**, W273-279.

Garrity, D. M., Childs, S. and Fishman, M. C. (2002). The *heartstrings* mutation in zebrafish causes heart/fin Tbx5 deficiency syndrome. *Development* **129**, 4635-4645.

Han, Y., Slivano, O. J., Christie, C. K., Cheng, A. W. and Miano, J. M. (2015). CRISPR-Cas9 genome editing of a single regulatory element nearly abolishes target gene expression in mice--brief report. *Arterioscler Thromb Vasc Biol* **35**, 312-315.

Hayashi, T., Sakamoto, K., Sakuma, T., Yokotani, N., Inoue, T., Kawaguchi, E., Agata, K., Yamamoto, T. and Takeuchi, T. (2014). Transcription activator-like effector nucleases efficiently disrupt the target gene in Iberian ribbed newts (*Pleurodeles waltl*), an experimental model animal for regeneration. *Dev Growth Differ* **56**, 115-121.

Hayashi, T. and Takeuchi, T. (2016). Mutagenesis in Newts: Protocol for Iberian Ribbed Newts. *Methods Mol Biol* **1338**, 119-126.

Hayashi, T., Yokotani, N., Tane, S., Matsumoto, A., Myouga, A., Okamoto, M. and Takeuchi, T. (2013). Molecular genetic system for regenerative studies using newts. *Dev Growth Differ* **55**, 229-236.

Hill, R. E. (2007). How to make a zone of polarizing activity: insights into limb development via the abnormality preaxial polydactyly. *Dev Growth Differ* **49**, 439-448.

Hill, R. E., Heaney, S. J. and Lettice, L. A. (2003). Sonic hedgehog: restricted expression and limb dysmorphologies. *J Anat* **202**, 13-20.

Hill, R. E. and Lettice, L. A. (2013). Alterations to the remote control of *Shh* gene expression cause congenital abnormalities. *Philos Trans R Soc Lond B Biol Sci* **368**,

20120357.

Hwang, W. Y., Fu, Y., Reyon, D., Maeder, M. L., Tsai, S. Q., Sander, J. D., Peterson, R. T., Yeh, J. R. and Joung, J. K. (2013). Efficient genome editing in zebrafish using a CRISPR-Cas system. *Nat Biotechnol* **31**, 227-229.

Inoue, T., Inoue, R., Tsutsumi, R., Tada, K., Urata, Y., Michibayashi, C., Takemura, S. and Agata, K. (2012). Lens regenerates by means of similar processes and timeline in adults and larvae of the newt *Cynops pyrrhogaster*. *Dev Dyn* **241**, 1575-1583.

Iten, L. E. and Bryant, S. V. (1973). Forelimb regeneration from different levels of amputation in the newt,*Notophthalmus viridescens*: Length, rate, and stages. *Wilhelm Roux Arch Entwickl Mech Org* **173**, 263-282.

Kanda, Y. (2013). Investigation of the freely available easy-to-use software 'EZR' for medical statistics. *Bone Marrow Transplant* **48**, 452-458.

Kim, S., Kim, D., Cho, S. W., Kim, J. and Kim, J. S. (2014). Highly efficient RNA-guided genome editing in human cells via delivery of purified Cas9 ribonucleoproteins. *Genome Res* **24**, 1012-1019.

Kistler, K. E., Vosshall, L. B. and Matthews, B. J. (2015). Genome engineering with CRISPR-Cas9 in the mosquito Aedes aegypti. *Cell Rep* **11**, 51-60.

Kmita, M., Tarchini, B., Zàkàny, J., Logan, M., Tabin, C. J. and Duboule, D. (2005). Early developmental arrest of mammalian limbs lacking HoxA/HoxD gene function. *Nature* **435**, 1113-1116.

Kuscu, C., Arslan, S., Singh, R., Thorpe, J. and Adli, M. (2014). Genome-wide analysis reveals characteristics of off-target sites bound by the Cas9 endonuclease. *Nat Biotechnol* **32**, 677-683.

Kvon, E. Z., Kamneva, O. K., Melo, U. S., Barozzi, I., Osterwalder, M., Mannion, B. J., Tissières, V., Pickle, C. S., Plajzer-Frick, I., Lee, E. A., et al. (2016). Progressive loss of function in a limb enhancer during snake evolution. *Cell* **167**, 633-642.e611.

Leal, F. and Cohn, M. J. (2016). Loss and re-emergence of legs in snakes by modular evolution of *Sonic hedgehog* and *HOXD* enhancers. *Curr Biol* **26**, 2966-2973.

Leone, M., Magadum, A. and Engel, F. B. (2015). Cardiomyocyte proliferation in cardiac development and regeneration: a guide to methodologies and interpretations. *Am J Physiol Heart Circ Physiol* **309**, H1237-1250.

Lettice, L. A., Devenney, P., De Angelis, C. and Hill, R. E. (2017). The conserved Sonic hedgehog limb enhancer consists of discrete functional elements that regulate precise spatial expression. *Cell Rep* **20**, 1396-1408.

Lettice, L. A., Heaney, S. J., Purdie, L. A., Li, L., de Beer, P., Oostra, B. A., Goode,

D., Elgar, G., Hill, R. E. and de Graaff, E. (2003). A long-range *Shh* enhancer regulates expression in the developing limb and fin and is associated with preaxial polydactyly. *Hum Mol Genet* **12**, 1725-1735.

Lettice, L. A., Williamson, I., Devenney, P. S., Kilanowski, F., Dorin, J. and Hill, R. E. (2014). Development of five digits is controlled by a bipartite long-range cis-regulator. *Development* **141**, 1715-1725.

Lettice, L. A., Williamson, I., Wiltshire, J. H., Peluso, S., Devenney, P. S., Hill, A. E., Essafi, A., Hagman, J., Mort, R., Grimes, G., et al. (2012). Opposing functions of the ETS factor family define *Shh* spatial expression in limb buds and underlie polydactyly. *Dev Cell* **22**, 459-467.

Li, D., Qiu, Z., Shao, Y., Chen, Y., Guan, Y., Liu, M., Li, Y., Gao, N., Wang, L., Lu, X., et al. (2013). Heritable gene targeting in the mouse and rat using a CRISPR-Cas system. *Nat Biotechnol* **31**, 681-683.

Lo, T. W., Pickle, C. S., Lin, S., Ralston, E. J., Gurling, M., Schartner, C. M., Bian, Q., Doudna, J. A. and Meyer, B. J. (2013). Precise and heritable genome editing in evolutionarily diverse nematodes using TALENs and CRISPR/Cas9 to engineer insertions and deletions. *Genetics* **195**, 331-348.

López-Martínez, A., Chang, D. T., Chiang, C., Porter, J. A., Ros, M. A., Simandl, B. K., Beachy, P. A. and Fallon, J. F. (1995). Limb-patterning activity and restricted

posterior localization of the amino-terminal product of Sonic hedgehog cleavage. *Curr Biol* **5**, 791-796.

Mescher, A. L. (1976). Effects on adult newt limb regeneration of partial and complete skin flaps over the amputation surface. *J Exp Zool* **195**, 117-128.

Naito, Y., Hino, K., Bono, H. and Ui-Tei, K. (2015). CRISPRdirect: software for designing CRISPR/Cas guide RNA with reduced off-target sites. *Bioinformatics* **31**, 1120-1123.

Nakayama, T., Fish, M. B., Fisher, M., Oomen-Hajagos, J., Thomsen, G. H. and Grainger, R. M. (2013). Simple and efficient CRISPR/Cas9-mediated targeted mutagenesis in *Xenopus tropicalis*. *Genesis* **51**, 835-843.

Nowoshilow, S., Schloissnig, S., Fei, J. F., Dahl, A., Pang, A. W. C., Pippel, M., Winkler, S., Hastie, A. R., Young, G., Roscito, J. G., et al. (2018). The axolotl genome and the evolution of key tissue formation regulators. *Nature*.

Parish, C. L., Beljajeva, A., Arenas, E. and Simon, A. (2007). Midbrain dopaminergic neurogenesis and behavioural recovery in a salamander lesion-induced regeneration model. *Development* **134**, 2881-2887.

Pinello, L., Canver, M. C., Hoban, M. D., Orkin, S. H., Kohn, D. B., Bauer, D. E. and Yuan, G. C. (2016). Analyzing CRISPR genome-editing experiments with CRISPResso.

Nat Biotechnol **34**, 695-697.

Pirotte, N., Leynen, N., Artois, T. and Smeets, K. (2016). Do you have the nerves to regenerate? The importance of neural signalling in the regeneration process. *Dev Biol* **409**, 4-15.

Rallis, C., Bruneau, B. G., Del Buono, J., Seidman, C. E., Seidman, J. G., Nissim, S., Tabin, C. J. and Logan, M. P. (2003). Tbx5 is required for forelimb bud formation and continued outgrowth. *Development* **130**, 2741-2751.

Ran, F. A., Hsu, P. D., Lin, C. Y., Gootenberg, J. S., Konermann, S., Trevino, A. E., Scott, D. A., Inoue, A., Matoba, S., Zhang, Y., et al. (2013). Double nicking by RNA-guided CRISPR Cas9 for enhanced genome editing specificity. *Cell* **154**, 1380-1389.

Riddle, R. D., Johnson, R. L., Laufer, E. and Tabin, C. (1993). *Sonic hedgehog* mediates the polarizing activity of the ZPA. *Cell* **75**, 1401-1416.

Roy, S. and Gardiner, D. M. (2002). Cyclopamine induces digit loss in regenerating axolotl limbs. *J Exp Zool* **293**, 186-190.

Roy, S., Gardiner, D. M. and Bryant, S. V. (2000). Vaccinia as a tool for functional analysis in regenerating limbs: ectopic expression of *Shh*. *Dev Biol* **218**, 199-205.

Sagai, T., Hosoya, M., Mizushina, Y., Tamura, M. and Shiroishi, T. (2005).

Elimination of a long-range cis-regulatory module causes complete loss of limb-specific *Shh* expression and truncation of the mouse limb. *Development* **132**, 797-803.

Sakane, Y., Iida, M., Hasebe, T., Fujii, S., Buchholz, D. R., Ishizuya-Oka, A., Yamamoto, T. and Suzuki, K. T. (2018). Functional analysis of thyroid hormone receptor beta in *Xenopus tropicalis* founders using CRISPR-Cas. *Biol Open* **7**.

Sakane, Y., Suzuki, K. T. and Yamamoto, T. (2017). A simple protocol for loss-of-function analysis in *Xenopus tropicalis* founders using the CRISPR-Cas system. *Methods Mol Biol* **1630**, 189-203.

Shapiro, M. D., Hanken, J. and Rosenthal, N. (2003). Developmental basis of evolutionary digit loss in the Australian lizard *Hemiergis*. *J Exp Zool B Mol Dev Evol* **297**, 48-56.

Shen, B., Zhang, J., Wu, H., Wang, J., Ma, K., Li, Z., Zhang, X., Zhang, P. and Huang, X. (2013). Generation of gene-modified mice via Cas9/RNA-mediated gene targeting. *Cell Res* **23**, 720-723.

Shi, D. L. and Boucaut, J. C. (1995). The chronological development of the urodele amphibian Pleurodeles waltl (Michah). *Int J Dev Biol* **39**, 427-441.

Shigeta, M., Sakane, Y., Iida, M., Suzuki, M., Kashiwagi, K., Kashiwagi, A., Fujii, S., Yamamoto, T. and Suzuki, K. T. (2016). Rapid and efficient analysis of gene function

using CRISPR-Cas9 in *Xenopus tropicalis* founders. *Genes Cells* **21**, 755-771.

Shin, H. Y., Wang, C., Lee, H. K., Yoo, K. H., Zeng, X., Kuhns, T., Yang, C. M., Mohr, T., Liu, C. and Hennighausen, L. (2017). CRISPR/Cas9 targeting events cause complex deletions and insertions at 17 sites in the mouse genome. *Nat Commun* **8**, 15464.

SINGER, M. and CRAVEN, L. (1948). The growth and morphogenesis of the regenerating forelimb of adult *Triturus* following denervation at various stages of development. *J Exp Zool* **108**, 279-308.

Singh, B. N., Doyle, M. J., Weaver, C. V., Koyano-Nakagawa, N. and Garry, D. J. (2012). Hedgehog and Wnt coordinate signaling in myogenic progenitors and regulate limb regeneration. *Dev Biol* **371**, 23-34.

Stocum, D. L. (2012). Regenerative biology and medicine.

Stocum, D. L. (2017). Mechanisms of urodele limb regeneration. *Regeneration (Oxf)* **4**, 159-200.

Stopper, G. F. and Wagner, G. P. (2007). Inhibition of Sonic hedgehog signaling leads to posterior digit loss in *Ambystoma mexicanum*: parallels to natural digit reduction in urodeles. *Dev Dyn* **236**, 321-331.

Suzuki, K. T., Isoyama, Y., Kashiwagi, K., Sakuma, T., Ochiai, H., Sakamoto, N.,

Furuno, N., Kashiwagi, A. and Yamamoto, T. (2013). High efficiency TALENs enable F_0 functional analysis by targeted gene disruption in *Xenopus laevis* embryos. *Biol Open* **2**, 448-452.

Suzuki, M., Yakushiji, N., Nakada, Y., Satoh, A., Ide, H. and Tamura, K. (2006). Limb regeneration in *Xenopus laevis* froglet. *ScientificWorldJournal* **6 Suppl 1**, 26-37.

Symmons, O., Pan, L., Remeseiro, S., Aktas, T., Klein, F., Huber, W. and Spitz, F. (2016). The *Shh* topological domain facilitates the action of remote enhancers by reducing the effects of genomic distances. *Dev Cell* **39**, 529-543.

Tanaka, E. M. (2016). The molecular and cellular choreography of appendage regeneration. *Cell* **165**, 1598-1608.

Thornton, C. (1956). The relation of epidermal innervation to the regeneration of limb deplants in *amblystoma* larvae. *Journal of Experimental Zoology* **133**, 281-299.

Tickle, C. (1981). The number of polarizing region cells required to specify additional digits in the developing chick wing. *Nature* **289**, 295-298.

Tickle, C., Summerbell, D. and Wolpert, L. (1975). Positional signalling and specification of digits in chick limb morphogenesis. *Nature* **254**, 199-202.

Torok, M. A., Gardiner, D. M., Izpisúa-Belmonte, J. C. and Bryant, S. V. (1999).

Sonic hedgehog (*shh*) expression in developing and regenerating axolotl limbs. *J Exp Zool* **284**, 197-206.

Tsutsumi, R., Inoue, T., Yamada, S. and Agata, K. (2015). Reintegration of the regenerated and the remaining tissues during joint regeneration in the newt *Cynops pyrrhogaster*. *Regeneration (Oxf)* **2**, 26-36.

Untergasser, A., Cutcutache, I., Koressaar, T., Ye, J., Faircloth, B. C., Remm, M. and Rozen, S. G. (2012). Primer3--new capabilities and interfaces. *Nucleic Acids Res* **40**, e115.

Urata, Y., Yamashita, W., Inoue, T. and Agata, K. (2018). Spatio-temporal neural stem cell behavior leads to both perfect and imperfect structural brain regeneration in adult newts. *Biol Open* **7**.

Wang, F., Shi, Z., Cui, Y., Guo, X., Shi, Y. B. and Chen, Y. (2015). Targeted gene disruption in *Xenopus laevis* using CRISPR/Cas9. *Cell Biosci* **5**, 15.

Wang, H., Yang, H., Shivalila, C. S., Dawlaty, M. M., Cheng, A. W., Zhang, F. and Jaenisch, R. (2013). One-step generation of mice carrying mutations in multiple genes by CRISPR/Cas-mediated genome engineering. *Cell* **153**, 910-918.

Williamson, I., Hill, R. E. and Bickmore, W. A. (2011). Enhancers: from developmental genetics to the genetics of common human disease. *Dev Cell* **21**, 17-19.

Wu, X., Scott, D. A., Kriz, A. J., Chiu, A. C., Hsu, P. D., Dadon, D. B., Cheng, A. W., Trevino, A. E., Konermann, S., Chen, S., et al. (2014). Genome-wide binding of the CRISPR endonuclease Cas9 in mammalian cells. *Nat Biotechnol* **32**, 670-676.

Yakushiji, N., Suzuki, M., Satoh, A., Sagai, T., Shiroishi, T., Kobayashi, H., Sasaki, H., Ide, H. and Tamura, K. (2007). Correlation between *Shh* expression and DNA methylation status of the limb-specific *Shh* enhancer region during limb regeneration in amphibians. *Dev Biol* **312**, 171-182.

Yang, Y., Drossopoulou, G., Chuang, P. T., Duprez, D., Marti, E., Bumcrot, D., Vargesson, N., Clarke, J., Niswander, L., McMahon, A., et al. (1997). Relationship between dose, distance and time in Sonic Hedgehog-mediated regulation of anteroposterior polarity in the chick limb. *Development* **124**, 4393-4404.

Yasue, A., Kono, H., Habuta, M., Bando, T., Sato, K., Inoue, J., Oyadomari, S., Noji, S., Tanaka, E. and Ohuchi, H. (2017). Relationship between somatic mosaicism of *Pax6* mutation and variable developmental eye abnormalities-an analysis of CRISPR genome-edited mouse embryos. *Sci Rep* **7**, 53.

Zhu, X., Xu, Y., Yu, S., Lu, L., Ding, M., Cheng, J., Song, G., Gao, X., Yao, L., Fan, D., et al. (2014). An efficient genotyping method for genome-modified animals and human cells generated with CRISPR/Cas9 system. *Sci Rep* **4**, 6420.

Zuo, E., Cai, Y. J., Li, K., Wei, Y., Wang, B. A., Sun, Y., Liu, Z., Liu, J., Hu, X., Wei, W., et al. (2017). One-step generation of complete gene knockout mice and monkeys by CRISPR/Cas9-mediated gene editing with multiple sgRNAs. *Cell Res* **27**, 933-945.